UNIVERSIDADE FEDERAL DE SANTA MARIA
CENTRO DE TECNOLOGIA
DEPARTAMENTO DE ENGENHARIA MECÂNICA
CURSO DE GRADUAÇÃO EM ENGENHARIA AEROESPACIAL

Alan Pitthan Couto

PRELIMINARY DESIGN OF A LUDWIEG TUBE AS AN EXPERIMENTAL FACILITY FOR AN LABORATORY OF COMPRESSIBLE FLOWS AT UFSM

Santa Maria, RS
2020

Alan Pitthan Couto

PRELIMINARY DESIGN OF A LUDWIEG TUBE AS AN EXPERIMENTAL FACILITY FOR AN LABORATORY OF COMPRESSIBLE FLOWS AT UFSM

Trabalho de Conclusão de Curso apresentado ao Curso de Graduação em Engenharia Aeroespacial, da Universidade Federal de Santa Maria (UFSM, Santa Maria/RS), como requisito parcial para obtenção do grau de **Bacharel em Engenharia Aeroespacial**. Defesa realizada por videoconferência.

ORIENTADOR: Prof. Dr. João Felipe de Araújo Martos

Santa Maria, RS
2020

Alan Pitthan Couto

PRELIMINARY DESIGN OF A LUDWIEG TUBE AS AN EXPERIMENTAL FACILITY FOR AN LABORATORY OF COMPRESSIBLE FLOWS AT UFSM

Trabalho de Conclusão de Curso apresentado ao Curso de Graduação em Engenharia Aeroespacial, da Universidade Federal de Santa Maria (UFSM, Santa Maria/RS), como requisito parcial para obtenção do grau de **Bacharel em Engenharia Aeroespacial**.

Aprovado em Outubro de 2020:

João Felipe de Araújo Martos, Dr. (UFSM)
(Presidente/Orientador)

Giuliano Demarco, Dr. (UFSM)

Paulo Gilberto de Paula Toro, Dr. (UFRN)

Santa Maria, RS
2020

AGRADECIMENTOS

Em primeiro lugar gostaria de agradecer à minha família, especialmente a minha mãe, Valeska por todo o apoio, amor incondicional e força que sempre teve não só enquanto eu desenvolvia este trabalho, mas por todos os anos da minha existência. Também, ao meu irmãozinho canídeo Zeca por afastar minha irritação e tristeza em alguns momentos. São ambos o meu porto seguro.

Ao meu orientador, Prof. João Martos, pela orientação e amizade durante estes últimos anos de graduação.

Aos meus colegas de curso, especialmente a Augusto, Fortunato, Jonas e Luiz com os quais criei grandes laços de amizade ao longo destes 5 anos, onde passamos por diversas situações tanto de alegria quanto de tristeza, sempre apoiando-nos mutuamente.

À Thalita e Carla pelo apoio e carinho singulares nos momentos difíceis ao longo de minha trajetória.

A Universidade Federal de Santa Maria e todos os professores do curso, pelas oportunidades e ensinamentos que moldaram minha trajetória acadêmica e impactaram no meu crescimento profissional ao longo da graduação.

RESUMO

PROJETO PRELIMINAR DE UM TUBO DE LUDWIEG COMO UM APARATO EXPERIMENTAL PARA UM LABORATÓRIO DE ESCOAMENTOS COMPRESSÍVEIS NA UFSM

AUTOR: Alan Pitthan Couto
ORIENTADOR: João Felipe de Araújo Martos

Túneis de vento pulsados são ferramentas utilizadas para reproduzir as condições necessárias para efetuar pesquisa e desenvolvimento que dependam de escoamentos com alto número de Mach. A replicação destas condições do escomento é crucial para o processo de validação de novas tecnologias aeroespaciais e a compreeensão de fenômenos complexos do escoamento. Um tubo de Ludwieg é um aparato experimental utilizado para replicar o ambiente encontrado em voos supersônicos e hipersônicos capaz de gerar uma ampla gama de escoamentos variando o número de Mach, número de Reynolds e entalpia, tornando-o em um dos dispositivos laboratorias mais versáteis para aplicações deste tipo. O objetivo deste trabalho é o projeto preliminar de um tubo Ludwieg planejado para ser instalado na Universidade Federal de Santa Maria (UFSM) como uma ferramenta de pesquisa e desenvolvimento para análise de escoamento compressível. Para tanto, é necessária a compreensão de cada um dos componentes do tubo de Ludwieg e seus aspectos teóricos a respeito dos escoamentos de alta velocidade gerados durante o funcionamento. A teoria de base de escoamento isentrópico quase-unidimensional foi utilizada para descrever o escoamento de alta velocidade gerado na seção de testes e para obtenção das condições de operação que influenciam no dimensionamento mecânico. Uma abordagem de engenharia de sistemas foi implementada na metodologia de projeto a fim de caracterizar os requisitos que orientam o desenvolvimento do sistema de interesse ao longo dos estágios iniciais do ciclo de vida. O projeto mecânico da seção do driver -seção de alta pressão e temperatura, foi conduzido de acordo com normas de projeto segundo a ASME. O dimensionamento preliminar da seção do driver, seção de teste e reservatório são apresentados. Instalações pulsadas operacionais em todo o mundo com características semelhantes são usadas como referência para o desenvolvimento e comparação de capacidades operacionais teóricas. Ao fim do trabalho foi concebido o projeto o preliminar do tubo de Ludwieg da UFSM.

Palavras-chave: Tubo de Ludwieg. Hipersônica. Pesquisa Experimental. Projeto Conceitual. Engenharia de Sistemas. Projeto Mecânico.

ABSTRACT

PRELIMINARY DESIGN OF A LUDWIEG TUBE AS AN EXPERIMENTAL FACILITY FOR AN LABORATORY OF COMPRESSIBLE FLOWS AT UFSM

AUTHOR: Alan Pitthan Couto
ADVISOR: João Felipe de Araújo Martos

Pulsed wind tunnels are tools used to reproduce the necessary conditions to perform research and development which depend of high Mach number flows. The replication of these flow conditions is crucial for the validation process of new aerospace technologies and the understanding of complex flow phenomena. A Ludwieg tube is an experimental apparatus used to replicate supersonic and hypersonic flight conditions, capable of generating a wide range of flows varying the Mach number, Reynolds number and enthalpy, making it one of the most versatile testing facilities for applications of this nature. The main objective of this work is the preliminary design of a Ludwieg tube planned to be installed at Universidade Federal de Santa Maria (UFSM) as a research and development tool for compressible flow analysis. Therefore, the understanding of each of the Ludwieg tube components and its theoretical aspects regarding the high-speed flows generated during operation is necessary. The basic theory of quasi-one-dimensional isentropic flow was used to describe the high-speed flows generated in the test section and to obtain the operating conditions which influence the mechanical project. A systems engineering approach was implemented into the project methodology in order to characterize the requirements that guide the development of the system of interest throughout the initial life-cycle stages. The mechanical design of the driver section - high pressure and temperature section, was carried out following ASME design standards. The preliminary design of the driver section, test section and dump tank are presented. Operational pulsed installations around the world with similar characteristics are used as a reference for the development and comparison of theoretical operational capabilities. In the end of the work, the preliminary project of the UFSM Ludwieg tube was conceived.

Keywords: Ludwieg Tube. Hypersonics. Experimental Research. Conceptual Project. Systems Engineering. Mechanical Project.

LIST OF FIGURES

Figure 1.1 – Concorde's last-ever flight on November 26, 2003. 14
Figure 1.2 – XB-1 prototype aircraft with fuselage and wings assembled. 15
Figure 1.3 – X-59 demonstrator. 15
Figure 1.4 – Brazilian 14-X waverider vehicle conceptual representation. 16
Figure 3.1 – Shock tunnel layout. 20
Figure 3.2 – T3 hypersonic shock tunnel. 20
Figure 3.3 – Expansion tube layout. 21
Figure 3.4 – Continuous wind-tunnel facility from NASA Ames Research Center. 22
Figure 3.5 – Ludwieg Tube layout. 26
Figure 3.6 – Detailed HTFD driver sections. 27
Figure 3.7 – Staged driver section with heating. 28
Figure 3.8 – PHLIC configuration concept. 28
Figure 3.9 – Prepared grooved diaphragm (left) and burst diaphragm after test run (right). 30
Figure 3.10 – Fast action valve component representation in a longitudinal cut view. .. 31
Figure 3.11 – Core flow region in a Mach number 6 contoured nozzle exit. 32
Figure 3.12 – T3 conical nozzle assembly (left) and modular nozzle throat section (right). 32
Figure 3.13 – Shockwave formation inside the diffuser. 34
Figure 3.14 – Representation of the Ludwieg tube test run. 36
Figure 4.1 – Generic life cycle project. 41
Figure 5.1 – Atmospheric air conditions change with altitude. 49
Figure 5.2 – Unit Reynolds number and altitude plot for different flight Mach numbers. 50
Figure 5.3 – Stagnation pressure requirements to replicate the exact real flight pressure conditions. 52
Figure 5.4 – Stagnation temperature requirements to replicate the exact real flight temperature conditions. 53
Figure 5.5 – Design of d_0 for different M_{DT} requirements. 54
Figure 5.6 – Analysis of flow quality for M_{DT} = 0.025. 55
Figure 5.7 – Analysis of flow quality for M_{DT} = 0.04. 56
Figure 5.8 – Analysis of stagnation conditions drop on test start. 57
Figure 5.9 – Allowable stress plots for aluminium (AL), carbon steel (CS) and stainless steel grades (SS) according to temperature. 60
Figure 5.10 – Allowable stress plot for steel grade SA312 TP304 according to temperature. 61
Figure 5.11 – Flange connection assembly in exploded view. 63
Figure 5.12 – Sylvania 18kW electrical air heater. 63
Figure 5.13 – Movable under-carriage supports, seen at the extremes of the driver length and test section. 64
Figure 5.14 – Sleeve assembly for the double diaphragm section. 65
Figure 5.15 – Test Section Concept 1. 67
Figure 5.16 – Dump Tank Concept 1. 68
Figure 5.17 – Test Section Concept 2. 68
Figure 5.18 – Dump Tank Concept 2. 69
Figure 5.19 – Test Section Concept 3. 69

Figure 5.20 – Operational Reynolds Envelope for the proposed Ludwieg tube. 71

LIST OF TABLES

Table 3.1 – Examples of known Ludwieg tubes. 25
Table 5.1 – Stakeholder needs. 43
Table 5.2 – Stakeholder Requirements 44
Table 5.3 – Project Requirements 46
Table 5.4 – Atmospheric air properties for specific altitude levels. 49
Table 5.5 – Temperature and pressure losses. 58
Table 5.6 – Proposed Ludwieg tube key parameters 59
Table 5.7 – Driver section main mechanical specifications. 62
Table 5.8 – Static temperatures, dynamic viscosity's and enthalpy levels for the attainable test section flows inside the Reynolds number Envelope. 71
Table 5.9 – Unit Reynolds range comparison with another Ludwieg tubes. 72
Table 5.10 – Unit Reynolds and dynamic viscosity for different altitude levels at Mach 5. 72

LIST OF ABBREVIATIONS AND ACRONYMS

$AFRL$ Air Force Research Laboratory

$ASME$ The American Society of Mechanical Engineers

BL Boundary Layer

CFD Computational Fluid Dynamics

DC Direct-connect

ESA European Space Agency

FJ Free-jet

$IEAv$ Institute for Advanced Studies

MOC Method of Characteristics

$NASA$ National Aeronautics and Space Administration

REQ Requirement

SOI System of Interest

STK Stakeholder

$T3$ Hypersonic Shock Tunnel T3

TRL Technology Readiness Level

TU Technical University

$UFSM$ Universidade Federal de Santa Maria

$USAFA$ United States Air Force Academy

$UTSA$ University of Texas San Antonio

LIST OF SYMBOLS

A	Cross-section area
A_{DT}	Driver cross-section area
$A*$	Nozzle throat cross-section area
b_i	Internal mechanical tolerance
C	Sutherland constant
c	Local sound speed
d_0	Driver internal diameter
d_2	Nozzle exit diameter
d_3	Test section internal diameter
e	Driver wall thickness
γ	Specific heats ratio
H	Altitude
h	Enthalpy
h_0	Stagnation enthalpy
L_{DT}	Driver section length
l_{max}	Maximum test model width
M	Mach number
M_{DT}	Driver section Mach number
μ	Dynamic viscosity
μ_{ref}	Reference dynamic viscosity
t	test time
P	Static pressure
P_0	Stagnation pressure
P_i	Pre-run pressure
R	Gas constant
Re	Reynolds Number
ρ	Density

ρ_0	Stagnation density
ρ_i	Pre-run density
$S.F.$	Safety factor
σ_{allow}	Allowable stress
σ_{max}	Maximum stress
T	Static temperature
T_0	Stagnation temperature
T_{DT}	Driver post-expansion temperature
T_i	Pre-run temperature
T_{ref}	Reference temperature
u	Flow speed
V_{DT}	Driver section hydraulic volume

CONTENTS

1 INTRODUCTION 14
2 OBJECTIVES AND JUSTIFICATION 18
3 BIBLIOGRAPHY REVIEW 19
3.1 PULSED WIND TUNNELS 19
3.1.1 Shock Tubes and Shock Tunnels 19
3.1.2 Expansion Tubes 21
3.2 CONTINUOUS SUPERSONIC WIND TUNNELS 22
3.3 WIND-TUNNEL CONCEPT SELECTION 23
3.4 INTRODUCING THE LUDWIEG TUBE 23
3.4.1 Ludwieg Tube Main Features 24
3.4.2 Ludwieg Tube facilities worldwide 25
3.5 LUDWIEG TUBE 26
3.5.1 Driver 26
3.5.2 Diaphragm 29
3.5.3 Fast Action Valve 30
3.5.4 Nozzle 31
3.5.4.1 Nozzle Contour Design 32
3.5.5 Test Section 33
3.5.6 Diffuser 34
3.5.7 Dump Tank 35
3.6 LUDWIEG TUBE OPERATION 35
3.6.1 Governing Equations 36
3.6.1.1 Quasi-Unidimensional Isentropic Compressible Flow 36
3.6.1.2 Isentropic Flow with Area Change 37
3.6.1.3 Area-Mach Relation 38
3.6.1.4 Energy Equation 39
3.6.1.5 Initial Driver Tube Conditions 39
4 METHODOLOGY 41
4.1 CONCEPT STAGE 41
4.2 DEVELOPMENT STAGE 42
5 RESULTS AND ANALYSIS 43
5.1 CONCEPT STAGE 43
5.2 DEVELOPMENT STAGE 46
5.2.1 Operation Requirements 48
5.2.1.1 High-Speed Flight Conditions 48
5.2.1.2 Reynolds number Similarity 49
5.2.1.3 Driver Tube Stagnation Conditions 51
5.2.1.4 Driver Tube Mach number 53
5.2.2 Mechanical Project 58
5.2.2.1 Key Parameters of the Facility 58
5.2.2.2 Material Selection 60
5.2.2.3 Components Mechanical Project 61
5.2.3 Reynolds number Envelope 70
6 CONCLUSION 73
BIBLIOGRAPHY 74

APPENIDX A – MUDGE DIAGRAM 78
APPENIDX B – CONCEPTUAL VIEW OF THE PROPOSED FACILITY 80

1 INTRODUCTION

According to Bertin and Cummings (2003) and Anderson (2003a), high-speed flows greater than sound speed are named supersonic until a rule of thumb limit where speeds exceed Mach number 5, then entering in the hypersonic regime. When trespassing this "frontier" distinct phenomena takes place, such as severe viscous interactions and entropy changes, high temperature heating of the fuselage caused by air friction and the change of the gas flow properties due to the presence of dissociation and ionization effects.

The related research fields in both supersonic and hypersonic flights have renewed interest in the current aerospace sector, especially in regard to the development of supersonic and hypersonic vehicles. There is a niche available for the use of these technologies in various applications, such as commercial aviation, defense and access to space. The interest can be seen through the initiative of several countries that have invested considerable human and financial resources in the development of their own projects or through international cooperation efforts and partnerships.

On commercial aviation, passenger and cargo transportation at supersonic and hypersonics speeds provide substantial flight time reductions, which is very appealing. Until nowadays it remains an empty niche in this sector capabilities since Concorde's last flight in 2003, Figure 1.1.

Figure 1.1 – Concorde's last-ever flight on November 26, 2003.

Source: Adapted from CNN Travel (2020).

Due to the opportunity of these types of services private companies alone such as Boom, or in consortia like between Boeing and Aerion, seek the development of supersonic commercial aircraft and conceivable services. These aircraft, aim to be used especially on

transoceanic flight routes, drastically reducing long travel duration times.

Among these companies, Boom is currently on an advanced progress on their prototype aircraft, the XB-1 (Figure 1.2), planned to make initial ground testings in October of this year and planned to begin first flight tests in 2021 (Boom, 2020).

Figure 1.2 – XB-1 prototype aircraft with fuselage and wings assembled.

Source: Adapted from Boom (2020).

Additionally, research linked to the reduction of the sonic boom, caused when an object crosses the sound barrier, may allow flight routes above the continents to be safely executed at supersonic speed. One of these surveys is represented by the X-59 Quiet Supersonic Technology (QueSST) experimental demonstrator vehicle under development by Lockheed Martin for Project Low Boom Flight Demonstrator, coordinated by the National Aeronautics and Space Administration (NASA), Figure 1.3. From the demonstrator's flights over the continent, ground perception data will be collected for future usage in the development of new regulation standards for supersonic commercial flight (NASA, 2020a).

Figure 1.3 – X-59 demonstrator.

Source: NASA (2020b).

In hypersonic flight there is the design of the waverider vehicles, scramjet unmanned engine-fuselage integrated aircraft, Figure 1.4. The waverider technology generates lift

from the high pressure region at the bottom of the vehicle due to an attached shock wave generated on high-speed atmospheric flight. The captured flow is further compressed by the engine inlet and entering the combustion chamber with desired conditions. Airbreathing scramjet propulsion systems provide better efficiency for atmospheric hypersonic flight (ROMANELLI et al., 2011; TORO et al., 2012).

Figure 1.4 – Brazilian 14-X waverider vehicle conceptual representation.

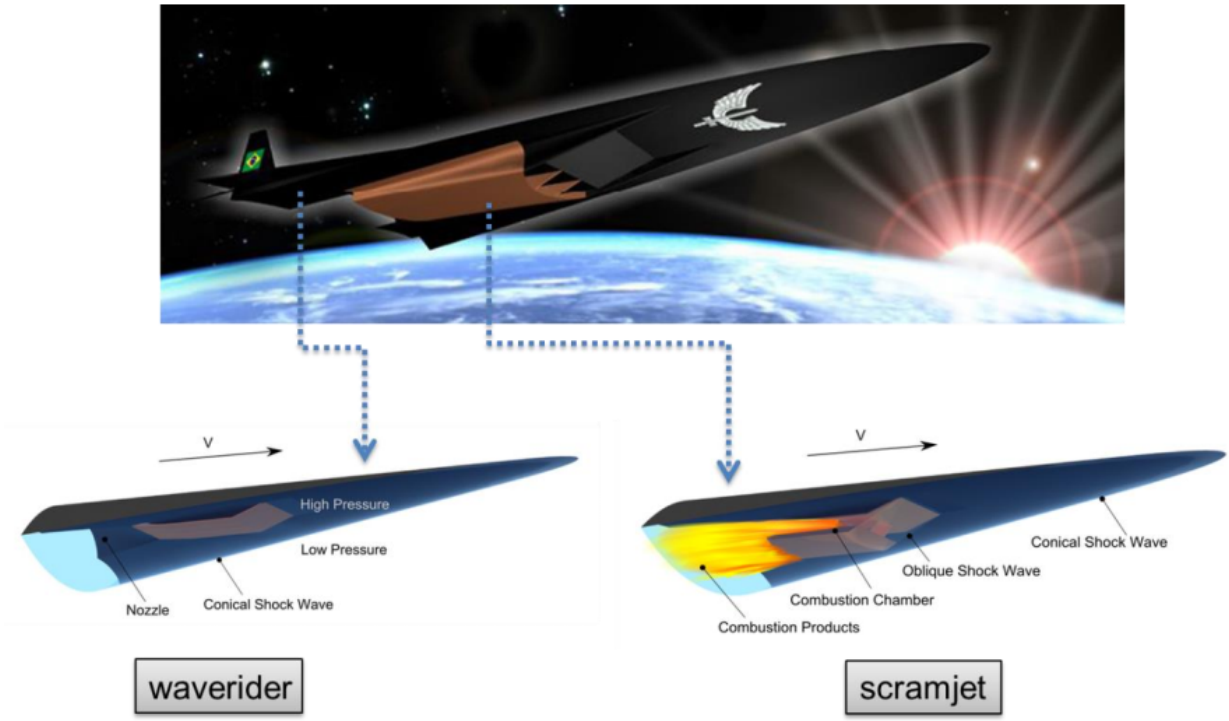

Source: Toro et al. (2012).

Beginning in the 1960's, many programs were created to verify scramjet systems. Among these, the National Aero-Space Plane (NASP) was an ambitious application for the scramjet propulsion in the development of a Single-Stage-to-Orbit (SSTO) platform for more cost-efficient space access. An hypersonic plane with multi-cycle propulsion capable to take-off in conventional runways, gain enough velocity to deliver payloads in orbit and return for landing. Capabilities foreseen to provide more efficiency and cut costs comparatively to traditional rocket launchers (BERTIN; CUMMINGS, 2003). However, despite the amount of developed technology as heritage from this particular project, its objective is still very far away from the necessary capabilities.

Still, even tough some programs did not succeed, the amount of research and resources invested in high-speed technologies since that time paved the way of the modern knowledge in this field, including the modern treatment of high-speed flows, aerothermodynamics and airbreathing propulsion systems (BERTIN; CUMMINGS, 2003).

Among some of these, it is possible to mention the HEXAFLY-INT program developed by the European Space Agency (ESA) in partnership with Russia, Australia and Brazil (CORDIS, 2020), and the X-51A airborne waverider demonstrator from the United States Air Force (USAF, 2011). Additionally, part of the scientific Brazilian development in hypersonics is related to the 14-X project, which is also characterized as a waverider aircraft (TORO et al., 2012). Also, studies related to hypersonic cruise, spacecraft atmosphere reentry on Earth and interplanetary exploration missions are also major research fields of great importance in hypersonics (BERTIN; CUMMINGS, 2003).

Due to the interest seen in the area, driven from all the advances obtained in these technologies and the quantity of active projects, it is possible to infer that in a near future high speed vehicles will be a reality in the aerospace sector and thus, the next aircraft generation will probably be hyper-fast. In addition, numerous related academic researches, such as the study of shock wave behavior, atmospheric re-entry of space vehicles, supersonic combustion and supersonic boundary layer are conducted worldwide due to the importance of the topic nowadays.

Despite the advanced state of modern computers and the quantity of enhanced multiphysics simulation softwares and solvers available, complex behaviors described by the fluid at high speeds are not yet fully understood even with the vast theoretical and experimental knowledge built on this field for several decades.

In this context, experimental installations capable of providing the desired conditions for high-speed flows in a controlled environment are fundamental for replicating high enthalpy flows and thermochemical phenomena present on high-speed flight, providing insight on the aerodynamic forces and momentum on scale models, provide benchmark data for verification of CFD solvers (CHAN et al., 2018) and testing and validation of new technologies. Among the types of existing experimental units, the Ludwieg tube has become one of the most chosen concepts of pulsed facilities employed by academic institutions around the world due to its versatility in simulating the supersonic and hypersonic regimes, low cost, ease of operation and simple design (BASHOR; COMBS, 2019).

The experimental devices for high-speeds testing available in Brazil consist of shock tunnels, all concentrated in the Laboratory of Aerothermodynamics and Hypersonics Prof. Henry T. Nagamatsu, at the Institute for Advanced Studies (IEAv), in São José dos Campos - SP. Even though Brazil is indeed included in the select group of countries that have part of their own research fields dedicated to high-speed flows, it is necessary to spread across the country new research centers and opportunities in academic institutions that contribute to the formation of specialized human resources on aerospace engineering. In this way, with the appropriate infrastructure and proper experimental apparatus for the academic environment, it is possible to boost the Brazilian scientific production and consequently the domain of these key technologies for national sovereignty in the future.

2 OBJECTIVES AND JUSTIFICATION

The primary objective of this work is the development of a preliminary project of a Ludwieg tube for academic research related to high-speed flows, which can be both used for national experimental research production in this field and for didactic purposes. This main objective is linked to secondary objectives of major relevance, described below.

First, identify needs and formulate requirements that the Ludwieg tube must accomplish concisely. With the entire process integrated to a system of interest (SOI) life-cycle initial stages as in a systems engineering method. The goal is to provide a terse project guidance, listing the variables taken into account and justification of the design choices under requirements constraints. These requirements were used to select the Ludwieg tube concept among the other types of pulsed wind-tunnels studied during the literature review. The selection

Second, demonstrate the analyzes applied to the key facility parameters - such as Mach number, driver Mach number, stagnation conditions, components dimensions, test-run duration, and understand their interactions with the sets of requirements as well as their impact into operational range, affordability and capabilities of the system.

Third, investigate similar current functional pulsed facilities aiming their design characteristics and experimental qualities, with the respective objectives of identifying possible trade-offs as well as insight of valid design choices. It is also done to evaluate the initial operational aspects obtained by the Ludwieg tube designed compared to existent ones.

The motivation of this work is to contribute for the development of an experimental apparatus to equip a future high-speed compressible flow laboratory at Universidade Federal de Santa Maria (UFSM), improving the infrastructure for experimental research and employing it as teaching tool for aerospace engineering students as well as related courses. Furthermore, this project is also carried out to provide insight about typical requirements associated to these facilities as a mean to approach one step closer to a reality where this, or other similar wind tunnels, can be conceived in other academic institutions in Brazil. This way, generating scientific and technological contributions for the high-speed flow field of knowledge along with the contributions to the aerospace sector in the country as well as training and specialization of human resources.

3 BIBLIOGRAPHY REVIEW

According to Chung (2015), experimental apparatus for testing high-speed flows can be divided into two groups: direct-connect (DC) and free-jet (FJ) facilities. DC units are used to simulate the flow conditions in the combustion chamber and the analysis of the combustion itself (fuel mixture, spark and flame). For such studies, the total pressure required to operate the facility is not too high. Usually the DC units provide a longer test time, however it is not possible to simulate the influence of the engine inlet on the experiment. FJ units, on the other hand, simulate the flow over the body surface, and from these it is possible to provide similarity of atmospheric flight conditions. However, it is necessary to store the test gas under higher pressure, which implies more robust installations. Furthermore, restrictions on available facility space and operating costs are limiting factors for testing time. Pulsed facilities can be used in both ways, depending in the adaptations made during the design phase.

3.1 PULSED WIND TUNNELS

Generating high-speed flows in laboratory demands high energy and a gas supply to generate the desired flow conditions. Those can be achieved, but due to most facilities constraints, the high-speed flows can be maintained just for a very small time period, between microseconds and milliseconds. Because of the short experimental run times, those facilities are known as pulsed wind tunnels. In the following subsections, some of the principal types of facilities apart from the Ludwieg tube are presented.

3.1.1 Shock Tubes and Shock Tunnels

The shock tube consists of a duct subdivided between a high pressure gas reservoir and another underlying low pressure section fulfilled with a test gas, named driver and driven respectively. Both sections are separated by a diaphragm employed as a physical barrier. When it suddenly breaks, the driver gas expands into the driven section, acting similarly as a piston, and a normal shock wave is generated, propagating through the test gas, which experiences strong accelerations and increase in its properties (pressure and temperature). At the same time a series of wave expansions travels upstream towards the driver end. Shock tubes are mainly used for thermodynamics and chemical equilibrium research on reactive flows, such as studies including gas dissociation rate, over test times in the scale of microseconds (IGRA; HOUAS, 2016; BRUN, 2011).

To Olivier (2016) and Gnemmi et al. (2016), the shock tunnel is derived from the shock tube, where a secondary thin diaphragm and a nozzle are integrated at the end of the driven (Figure 3.1), where the gases expand and the flow accelerates to a given design Mach number. Shock tunnels employ different gases in the upstream sections. The driver is filled with a light gas, such as helium, and the driven test gas is dry air. Downstream the nozzle there is a reservoir for the capture of gases in addition to the testing section, where a scale model can be placed. The testing time is still very short, in hundreds of microseconds even for large installations due to the high Mach numbers generated.

Figure 3.1 – Shock tunnel layout.

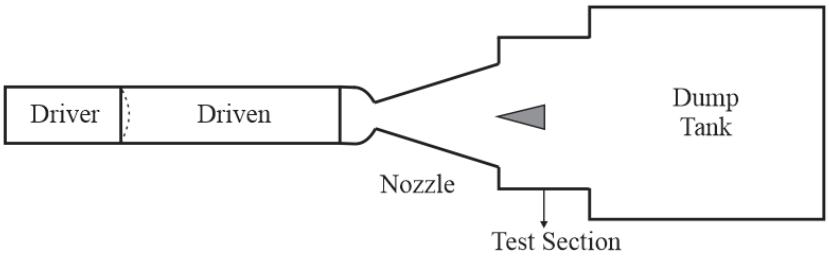

Source: Adapted from Gnemmi et al. (2016).

Current pulsed wind tunnels used for experimental research in Brazil consist of shock tubes and shock tunnels, present at the Laboratory of Aerothermodynamics and Hypersonics Prof. Henry T. Nagamatsu, at the Institute for Advanced Studies (IEAv), in São José dos Campos - SP. Namely, the apparatus are: T1 shock tube, T2, T3 and T4 shock tunnels, with the T3 being the one developed more recently and consisting as the largest one regarding test section size, Figure 3.2.

Figure 3.2 – T3 hypersonic shock tunnel.

Source: Romanelli et al. (2011).

3.1.2 Expansion Tubes

According to Gildfind, Morgan and Jacobs (2016), the expansion tube uses a similar configuration as the shock tube, however a thin second diaphragm is inserted at the end of the driven and this is followed by the acceleration tube, a long section filled with air at very low pressures. This additional section provides the facility with the capability to generate a wide range of hypervelocity flow conditions which, otherwise, would require very harsh stagnation requirements. In accordance with Bakos and Erdos (1995), the expansion tube is not structurally limited by these parameters, since the test gas is not stagnant. Additionally, a free-piston system is used for compression of the driver gas (such as helium), achieving very high pressure and temperature levels. Such that, the driver gas bursts the primary diaphragm. In the sequence, a strong shock travels through the test gas accelerating and compressing it.

The apparatus has this name due to the unstable expansion process in the acceleration tube, with the sudden change in conditions encountered by the wave-front. Inside the acceleration tube, the flow reaches speeds of up to 20km/s. Because of the high operational hypersonic Mach numbers, the applicability of the device is used, as an example, for simulating atmospheric reentry conditions (KLICHE; MUNDT; HIRSCHEL, 2011). Regarding with the expansion tube features, its concept allows to achieve the highest level of total pressure for chemically clean -dismissing the use of combustion reactions, high enthalpy flows, but trading-off in the shortest test time duration from comparatively with the other facilities, in the order of 1 millisecond (GILDFIND; MORGAN; JACOBS, 2016). The described parts of the system are illustrated in Figure 3.3.

Figure 3.3 – Expansion tube layout.

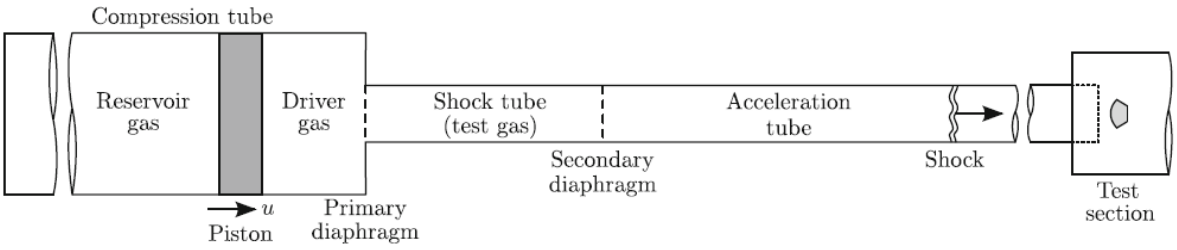

Source: Adapted from Gildfind, Morgan and Jacobs (2016).

3.2 CONTINUOUS SUPERSONIC WIND TUNNELS

Finally, there are also the continuous flow facilities used for tests with large-scale models and capable to supply high-speed flows for the duration of minutes. However, a complete infrastructure on a large, dedicated scale is required for this purpose. Due to the cost involved in the implementation and operation of these facilities they are impractical for construction in an academic environment. Only a few of them exists around the world. Figure 3.4 illustrates the continuous wind-tunnel installation from NASA Ames Research Center (ANDERSON, 2003a).

Figure 3.4 – Continuous wind-tunnel facility from NASA Ames Research Center.

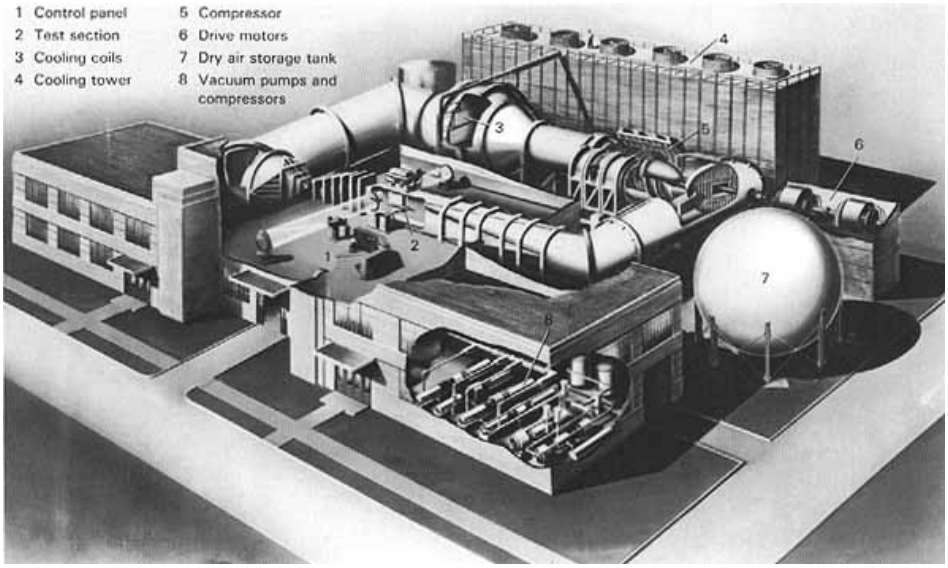

(a) Installation plant.

(b) Test section with large scale model.

Source: Adapted from Anderson (2003a).

3.3 WIND-TUNNEL CONCEPT SELECTION

As it is already know by the title of this work, the Ludwieg tube was the selected wind-tunnel concept for this project. It was chosen in accordance with needs that were formulated for the facility or, in other words, expected characteristics and capabilities of the system in order to extract the better possible use of it. A methodology analogous to a systems engineering approach was implemented to this work, which in the first step establishes a set of stakeholder needs that guide the main concept selection inside the initial life-cycle stage of the system. This methodology, needs and justifications are better specified and discussed in the Results Chapter. However, for the sake of clarity and logical order, this subject is also brought here. Along the 5 needs formulated, one of them and a specified design Mach number -that apply for the Ludwieg tube, were judged as fundamental and sufficient to choose this concept:

- **Low-cost of operation.**
- **Operational design at Mach 5.**

Fortunately, this concept also present a series of features - presented in the next section, that can be exploited to intensify the research potential of the facility and their benefits among the academic environment.

Concluding, it is good to clarify that each type of high-speed wind-tunnel have their own operational characteristics. First of all, the concept choice must agree with the desired needs or demands that are foreseen for the facility, identified as stakeholder needs (i.e. Mach number range, types of research and costs). The Ludwieg tube presents as a viable choice for Mach number ranges between low supersonic until around Mach 10 - maximum value seen for the facilities studied. The test section flow for a "standard" Ludwieg tube configuration - without using free-piston compression, is cold, near or below 273 K, as a result of the isentropic expansion of the test gas in the nozzle. The cold temperature is a limitation for research regarding combustion and other chemical processes. However the facility still manages to be useful for a wide set of fundamental high-speed aerodynamics research. All this characteristics are further discussed along this work.

3.4 INTRODUCING THE LUDWIEG TUBE

As exposed in Radespiel et al. (2016), even with several decades of scientific contributions in the study of hypersonic flows, the flow physics behaves in a complex way, and only the theoretical and numerical models are insufficient to predict the fluid behavior. Therefore, experimentation is crucial to fulfill the existent gaps and learn the processes.

However, it is still difficult to simulate the high speed and the high enthalpy levels that must occur realistically in high-speed flows. The extreme thermal loads and kinetic energy rate that follow the enthalpy levels achieved in hypersonic flight can only be fully generated in a few installations worldwide. And, it comes with the penalty of high operating costs and a short test times. Because of the challenges bounded to that, many experimental hypersonics research tend to be done on pulsed facilities that at least the Mach number and Reynolds number can be properly achieved, but with lower enthalpy levels.

In addition to that, according to Cummings and Mclaughlin (2012), hypersonic ground-based facilities are traditionally expensive to operate and maintain. The operation cost factor is one of the main obstacles to extensive academic research in hypersonic, such as the replacement of the test gases, usually light and inert gases are used for the FJ units described - which are used to deliver a strong shockwave in the test gas in order to attain the high-temperature requirements (GNEMMI et al., 2016), and the support infrastructure.

Resuming this scenery, the Ludwieg tube was introduced as an novel pulsated high-speed facility configuration in agreement to some top-level requirements which illustrates its potential, (RADESPIEL et al., 2016):

- Range of Mach numbers high enough to replicate typical hypersonic flow behaviours for blunt and slender configurations.
- Provide Reynolds number in order of 15×10^6 based on model scale to simulate of both laminar and turbulent flows.
- Test times as high as 100 milliseconds to enable the usage of many flow measurements techniques.
- Provide affordable operational costs.

3.4.1 Ludwieg Tube Main Features

Compared to the other pulsated facilities the Ludwieg tube presents the following advantages (RADESPIEL et al., 2016; KIMMEL et al., 2016; CUMMINGS; MCLAUGHLIN, 2012):

- Simple design and minimal support infrastructure required.
- Generation of extremely clean and high quality flows.
- Generation of high-speed flow conditions using only dry air as test gas, dismissing the use of inert gases such as helium.
- Longer test times in the order of 100 milliseconds.

- The higher test time enables the use of valve instead of consumable diaphragms further reducing the operation costs and the time interval between shots.

3.4.2 Ludwieg Tube facilities worldwide

Due to the performance and the advantages inherent to the Ludwieg tube configuration, many academic institutions and research centers around the world employ the device. A list of some of the known facilities is showed below, with their specifications of affordable Mach number (M) and test section diameter, Table 3.1:

Table 3.1 – Examples of known Ludwieg tubes.

Facility Name	**Location**	**Specifications**
RWG	DNW Göttingen, Germany	*M = 2.9 to 6.9* *0.50m diameter test section*
Ludwieg Tube	Caltech, USA	*M = 2.3* *0.2m x 0.2m test section*
Boeing/AFOSR Quiet Tunnel	Purdue University, USA	*M = 6* *0.24m diameter test section*
TUSQ	University of Southern Queensland, Australia	*M = 6* *0.22m diameter test section*
HHK	TU Braunschweig, Germany	*M = 6 to 11* *0.50m diameter test section*
YT1 Tube	Central Aerohydrodynamic Institute, Russia	*M = 5 to 10* *0.50m diameter test section*
USAFA	US Air Force Academy, USA	*M = 6* *0.50m diameter test section*
AFRL	Air Force Research Laboratory, USA	M = 6 1.2m diameter test section

Source: (KIMMEL et al., 2016; CUMMINGS; MCLAUGHLIN, 2012; KOPPENWALLNER, 2000; DAVID et al., 2006; WIDODO; BUTTSWORTH, 2010).

After the investigation on some Ludwieg tubes employed by preeminent academic institutions it is clear that this unit consists of a popular experimental apparatus and has several advantages in comparison to other FJ pulsed wind-tunnels units. In special, the affordability of this type of facility and the available test time, compared to others are the main attributes.

3.5 LUDWIEG TUBE

A standard Ludwieg tube layout consists in a high-pressure gas reservoir, called driver, followed by a test-run trigger component, nozzle, test section, diffuser and a dump tank, Figure 3.5. The stagnated gas is maintained inside the driver tube by a physical barrier upstream the nozzle entrance that can be a diaphragm or a fast action valve. When this barrier is suddenly removed it triggers the hypersonic flow generation into the test section (BASHOR et al., 2019).

Figure 3.5 – Ludwieg Tube layout.

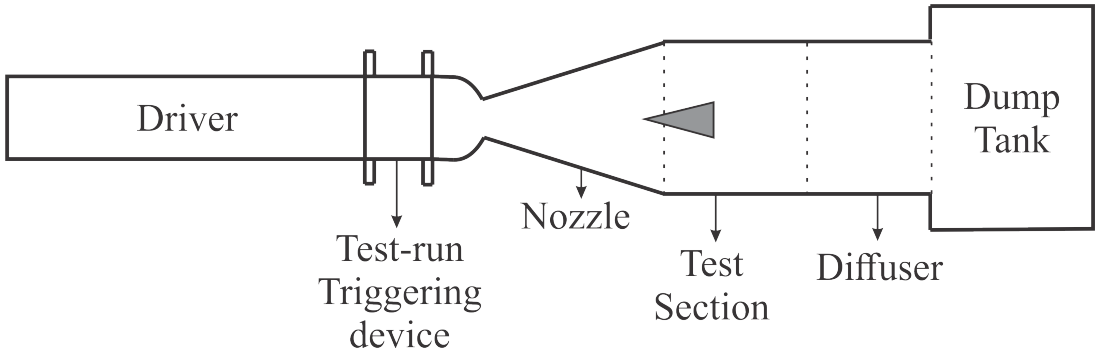

Source: Adapted from Radespiel et al. (2016).

3.5.1 Driver

According to Bashor and Combs (2019), in the driver section there is the storage of gas under high pressure and temperature stagnation conditions, responsible for the driving force of the experiment, recreate the desired flight conditions in the test section and also necessary to achieve high values of Reynolds. The existence of these conditions allows to conduct aerothermodynamic analyzes more accurately. The test gas used is atmospheric air itself, processed by a dryer and pumped by a compressor prior to the testing. As mentioned before, the dry air as test gas is another aspect that drastically influences the low cost of operating this facility. Special test gases, such as helium, are expensive and demand gas purification units in order to control the test gas composition.

The test time is directly influenced by the driver length, it is approximately the time spent by a expansion wave moving at the local sound speed to travel twice the driver length (Caltech, 2014). For this reason, even for facilities with a small test chamber, the driver section alone is usually composed by tens of meters of piping in order to attain the maximum affordable test-run duration. An alternative usually employed to circumvent laboratory physical restrictions is the use of elbow connections and curved sections. The HTFD Ludwieg

tube at TU Delf presented by Schrijer and Bannink (2010) uses a 29 m long driver divided into three individual sections, Figure 3.6, reducing the size of the facility.

Figure 3.6 – Detailed HTFD driver sections.

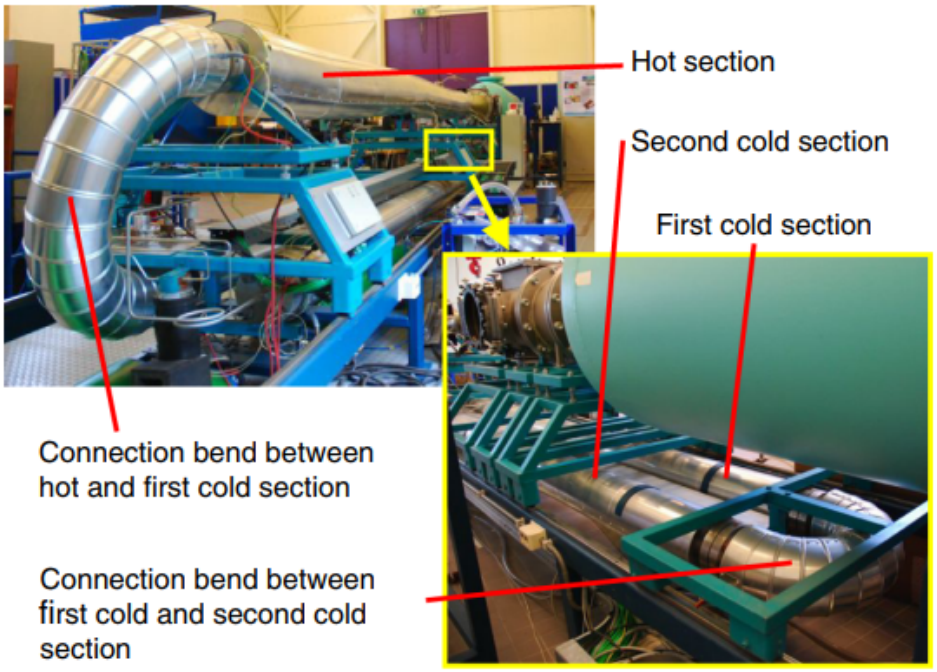

Source: Schrijer and Bannink (2010).

As pointed by Radespiel et al. (2016), the expansion process in the nozzle drastically reduces the static temperature of the gas. When the high speed flow crosses the divergent section of the nozzle, the gas expansion process occurs, where its internal energy in the form of temperature and pressure is converted into kinetic energy. As a result the test gas can fall below the saturation curve, or the condensation limit. This sudden drop in temperature can lead to the formation of ice on the instruments and the freezing of the gas, impairing the data collection and the realism of the experiment. To avoid this phenomenon the gas should be heated previously in the driver. So, electrical devices are employed for that, such as insulated heating tapes, heating cables or resistors are used around a portion or in the whole driver length.

Fundamentally, the operation costs of the Ludwieg tube will be represented by the energy consumed by the heating devices and auxiliary laboratory equipment. One way to reduce heating costs is to fix the heating tapes only in the portion of the driver that contains the mass of gas effectively consumed during the experiment - called hot slug. However, as explained by Koppenwallner, Müller-Eigner and Friehmelt (1993) and Schrijer and Bannink (2010), the heated section promotes an internal thermal gradient that must be compensated by the variation of the driver diameter in the following section in order to avoid disturbances in the flow with the expansion wave passage, i.e. the expansion wave reflection. The

phenomenon can be offset by the conservation of mass flow between both regions, as the flow velocity changes following the duct diameter. The conservation of the mass flow in the staged driver, Figure 3.7, is given by,

$$\frac{D_1}{D_2} = \left(\frac{T_2}{T_1}\right)^{0.25} \tag{3.1}$$

which represents an increase in the upstream piping diameter.

Figure 3.7 – Staged driver section with heating.

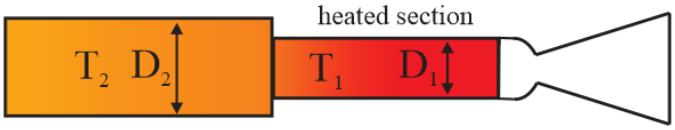

Source: Author.

However, for higher Mach numbers the stagnation conditions for real flight simulation cannot be fully achieved by electrical heating. In this way, some installations employ adiabatic gas compression carried out by the movement of a piston coupled in an additional upstream section from the driver, called compression tube, Figure 3.8. The free piston compression system as present on the T4 shock tunnel at Queensland University provides the high pressure and temperature stagnation levels while also maintaining the flow clean - without using chemical reactions or combustion processes to do so. The Pre-Heated Ludwieg Tube with Isentropic Compression (PHLIC) configuration is described by Chung (2015) and Chung, Houim and Laurence (2015).

Figure 3.8 – PHLIC configuration concept.

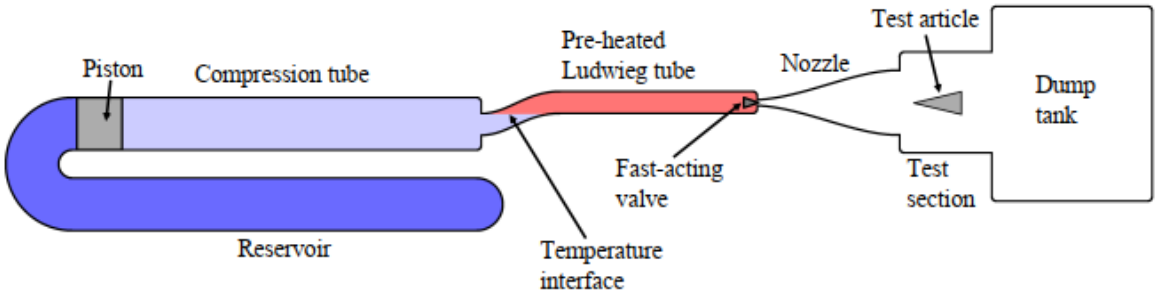

Source: Adapted from Chung, Houim and Laurence (2015).

3.5.2 Diaphragm

According to Hoffman and Combs (2019), the beginning of the experiment occurs when the gas from the driver is accelerated through the nozzle. This occurs from the rupture of a diaphragm or the opening of a valve, exposing the stagnated high pressure gas to the low pressure region downstream. This pressure gradient then drives the flow.

The diaphragms are usually fixed at the end of the driver tube. Although some pulsated facilities can use the diaphragm downstream the test section such as in the GALCIT Ludwieg tube. One advantage of this design is that a quieter flow can be produced, (Caltech, 2014).

The burst pressure is defined according to the base material used for manufacture, ranging from different grades of steel, aluminium or composites such as Mylar. Diaphragms can be used in two ways: a single diaphragm with only a single rupture disc or double diaphragm assembly, called buffer. The single diaphragm is coupled between flange connections, and its rupture can occurs simply when the pressure of the test gas reaches the burst pressure or by the actuation of a puncturing mechanism. As for the double diaphragm, after the apparatus is integrated, the duct region between the discs is pressurized to a value below the burst point. The pressure gradient between both inhibits the rupture of the set while the driver stagnation conditions are still been set. Then, the test is started by depressurizing the region between the discs, triggering the rupture. Among both types, the double diaphragm provides a better rupture control.

One of the critical requirements of this component is to prevent the loosening of splinters during rupture, as the high speed fragments can damage the instrumentation or other parts of the structure, as experienced by Martos (2014).

A procedure done into the components to both ensure flow quality after rupture and prevent fragmentation is machining crossed grooves on one of the diaphragm faces. The grooves will help guiding the diaphragm aperture in "petals" shape. The grooved face shall be positioned facing the lower pressure side (MARTOS, 2014). Figure 3.9 presents diaphragms before and after a test run.

For Kimmel et al. (2016), another way around the diaphragm fragmentation problem is positioning the part after the test section, however there are other associated disadvantages such as the need to charging the pressure from the driver until the test section.

Figure 3.9 – Prepared grooved diaphragm (left) and burst diaphragm after test run (right).

Source: Martos (2014).

3.5.3 Fast Action Valve

Many modern Ludwieg tubes feature a quick-acting valve replacing the diaphragm, or are designed to use both. According to Radespiel et al. (2016) the use of a valve allows to minimize the operations costs as does not consume diaphragms at every test. Diaphragms are usually cheap, so the main advantages regarding its exchange for a fast action valve, is to eliminate the risks associated to loosen fragments and an enhanced test-run control. The fast action valve design presented by Koppenwallner, Müller-Eigner and Friehmelt (1993), Figure 3.10, is adopted by several facilities.

According to Lindorfer et al. (2016), since the 1990's a number of Hoscschal-Hyperschall-Kanal (HHK) Ludwieg tubes designed by Hyperschall Technologie Göttingen research company employs fast-acting valves. The facilities currently operate at some universities in Europe such as University of Bremen, Technical University (TU) of Delft (the DEFLT Ludwieg tube mentioned previously), TU Dresden and TU Braunschweig, as well as the Mach 6 Ludwieg tube from USAFA at United States. This information is relevant since the component was not found at market by the research done during this work.

The operation principle of the valve consists of a piston aligned to the flow direction, whose pneumatic actuation is done by controlling the back pressure behind the piston, inside the piston housing. In the closed configuration, the piston docks near the nozzle throat blocking the flow passage (RADESPIEL et al., 2016).

For this, according to Cummings and Mclaughlin (2012), the piston is locked in place by the driver pressure which is transmitted by a bypass valve and a control tube behind the piston body. The piston is quickly opened by closing the bypass valve and opening an exhaust valve via a computer command. This system allows the valve opening time as fast as 10 milliseconds.

Figure 3.10 – Fast action valve component representation in a longitudinal cut view.

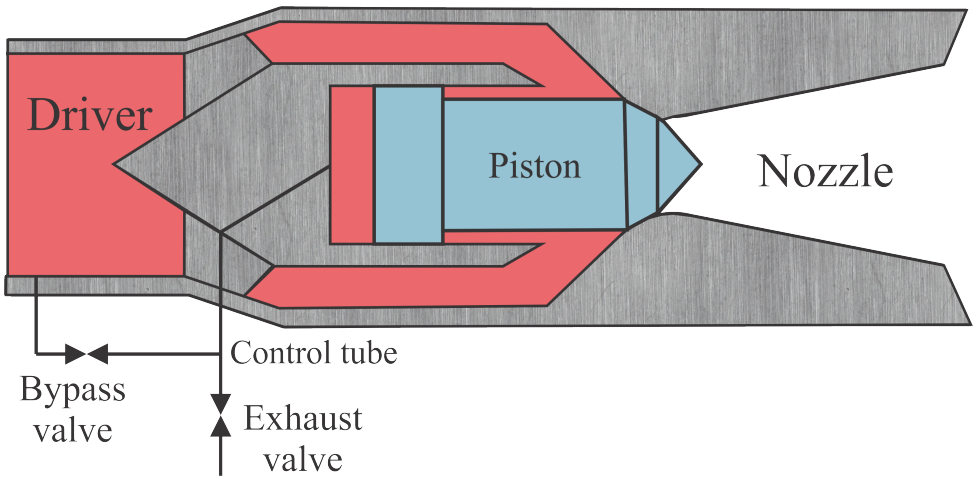

Source: Adapted from Radespiel et al. (2016).

3.5.4 Nozzle

The nozzle is designed to accelerate the flow from stagnation conditions to the desired Mach number, controlled by the the area ratio relation between the throat and nozzle exit cross sections (ANDERSON, 2003a). Some facilities are designed to cover a range of Mach numbers, for that the nozzle section is designed in a modular way to be easily replaced.

The nozzle configuration used in the Ludwieg tube is a convergent-divergent nozzle, or De Laval nozzle. In the convergent section, the flow is accelerated almost from rest to sonic regime and then in the divergent section accelerated to high-speeds. The efficient operation of the nozzle depends of the existent pressure ratio in the system to drive the gas. For this matter, the internal gas of the downstream sections after the driver is removed by vacuum pumps in order to minimize the back-pressure. This helps to reduce the pre-run driver requirements to achieve the desired test conditions (ANDERSON, 2003a).

In consequence of the low pressure at the nozzle exit, the flow will exit at the under-expanded condition. For this matter, it is a good practice to adjust the nozzle exit diameter to be less than the test section cross section so the remaining expansion process can develop away from the model. Due to the expansion and viscous effects near the walls the useful region where the desired test conditions are achieved are concentrated near the test section centerline. This region is known as the core flow region. In the CFD Mach number colormap results obtained from Radespiel et al. (2016) Mach number 6 nozzle is possible to visualize the core flow region, Figure 3.11.

Figure 3.11 – Core flow region in a Mach number 6 contoured nozzle exit.

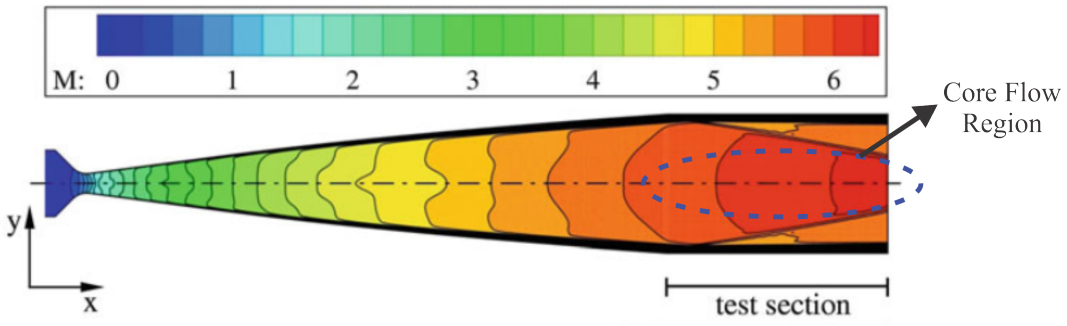

Source: Adapted from Radespiel et al. (2016).

3.5.4.1 Nozzle Contour Design

Conical nozzles present the same wall angle through the whole length, thus are simple to manufacture. A 15° half angle is a standard choice for conical nozzle design as the component does not become very long and the exit Mach number is attained. For instance, the T3 shock-tunnel employs a 15° half-angle conical nozzle with interchangeable throats for Mach numbers ranging from 6 to 25. The expansion section is segmented in four different pieces fabricated with medium carbon steel and aluminium, Figure 3.12 (TORO et al., 2006).

Figure 3.12 – T3 conical nozzle assembly (left) and modular nozzle throat section (right).

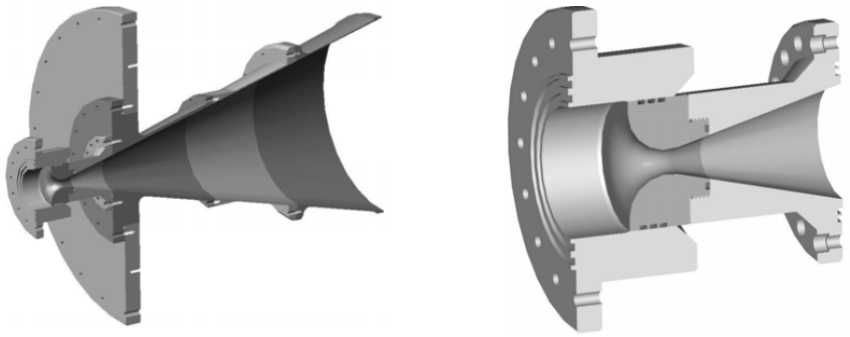

Source: Adapted from Toro et al. (2006).

The main issue of this design is related to nonparallel velocity components at the exit area that causes performance losses. Bell shaped nozzles or De Laval nozzles were developed to further increase performance giving more uniformity for the exit flow (SINGH, 2015).

These contoured nozzles are often obtained through the Method of Characteristics (MOC). The generation of a smooth contour propitiates the expansion process through

small expansion waves and uniformity of the streamlines at the exit area. Low intensity compression waves might propagate within the flow, however the idealised MOC is set to cancel this energy dissipation and propitiates the expansion process occurs with minimum losses (MURNAGHAN, 2019).

The ideal nozzle produces uniform parallel flow at exit and the expansion process occurs isentropically. The maximum thrust is generated with the exit pressure is designed to match the ambient pressure (SINGH, 2015). Those factors (flow uniformity and maximum thrust) are translated into better flow quality for high-speed wind tunnels and performance increase for aerospace vehicles. However ideal nozzles are typically very long due the low angle variation induced to not disturb the flow. Because of that, these nozzles are not much feasible for practical applications because of their high manufacture cost and weight. Propulsion systems instead prefer to use truncated nozzles or even conical nozzles, but they would typically produce poor flow quality.

The nozzle length problem was mitigated with the aid of optimization techniques, as the method developed by Rao (1958), employing Lagrangian multipliers together with MOC while keeping a fixed nozzle length as a design constraint. Components designed by this method are referred to as thrust optimized contour (TOC) nozzles.

The coupling of MOC and optimization is a powerful tool for hypersonic facilities nozzles as the flow quality requirement will impact experimental research. The MOC/BL is another method developed to monitor the growth of the boundary layer along the nozzle walls. The boundary layer becomes thicker at the exit area which tends to reduce the effective area, choking the flow, and lowering the attainable Mach number. However this particular method loses accuracy for higher Mach number regimes where the boundary layer becomes continuously thicker.

A novel design method was introduced to enhance even more the nozzle design for pulsed wind tunnels, by the coupling of CFD solver with optimization algorithms. The Navier-Stokes equations propitiate to compute interactions between core flow and boundary layer. This way the minimization flow angularity and Mach number deviation leading to very high quality flow (CHAN et al., 2018). Also, geometric constraints such as throat diameter and nozzle length can be added, which lead to more flexibility on design and the development of compact nozzles. One of the challenging aspects of this methodology however is the massive computational power and time required to perform the simulations.

3.5.5 Test Section

The test section is where the scale models and data gathering instrumentation are positioned and exposed to the high-speed flow. For that, it shall have adequate room size. Also, as pointed by Martos (2014) larger diameter test sections provide that the reflected

shock waves generated on the test section walls occur far from the model, providing a clear flow visualization and reliability of the experimental results.

The section is designed with hatched windows on all sides and supports for positioning sensors and probes. A common window configuration consists on two lateral opposite windows which can be used for schlieren imaging and a top window for infrared non-intrusive measurements (RADESPIEL et al., 2016). According to Kimmel et al. (2016), specifically for the tasks mentioned, fused silica transparency and calcium fluoride compositions can be used into the windows, respectively. Access ports for wiring and maintenance are also factors taken in account.

3.5.6 Diffuser

According to Anderson (2003b), the diffuser has the function of slowing the flow after the test section in order to have the lowest possible total pressure loss. Also, preventing the flow from reflecting and the downstream end and returning to the test section. This is done by compressing the flow via a sequence of oblique shock waves, terminated by a normal low intensity shock wave. The deceleration of the supersonic flow in the diffuser is done by its convergent geometry in the inlet which causes a sequence of oblique shock to form at the straight section, terminated by normal shock wave at the end, on which the flow becomes subsonic. The diffuser operation schematic can is shown in Figure 3.13. Some pulsed facilities dont't actually have a diffuser. In theses cases the flow is simply terminated when entering the dump tank and expanding inside the sudden volume increase

Figure 3.13 – Shockwave formation inside the diffuser.

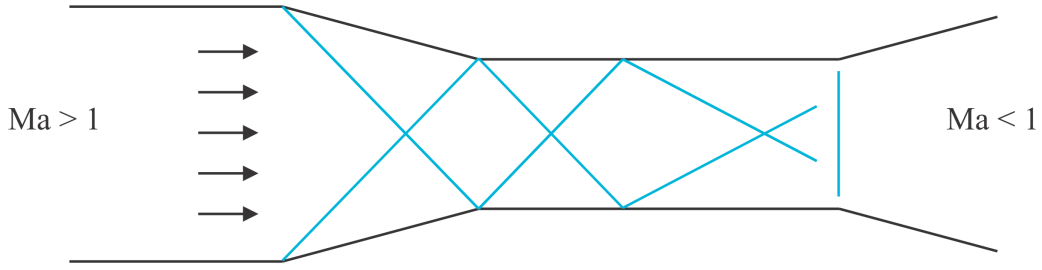

Source: Adapted from Anderson (2003b).

For Radespiel et al. (2016), another task of the diffuser is to increase the static pressure downstream the test section to prevent an early flow break caused by increasing pressure of the dump tank as it is fulfilled with the test gas.

3.5.7 Dump Tank

The dump tank is the final volume that stores the gas consumed during the whole operation time. The volume is designed in order to maintain the final equilibrium pressure after test-runs as close as possible to the atmospheric pressure. Vacuum pumps are essential laboratory support equipment's usually connected to the dump tank and are used to purge the internal gases from the downstream section, lowering the back-pressure before each experiment. The smaller the back-pressure obtained, the lower the pressure required on the driver to generate the high-speed flow (ANDERSON, 2003b).

3.6 LUDWIEG TUBE OPERATION

After the diaphragm rupture or the fast valve opening, a shock wave is generated that produces the desired flow conditions in the test section (LINDORFER et al., 2016). According to Chung (2015) and Caltech (2014), simultaneously an expansion wave is also generated, travelling upstream at the local speed of sound towards the driver end. The wave undergoes a reflection upon reaching the end wall, reversing its motion. Another reflection then occurs when the wave reaches the nozzle entrance and the process start again. This dynamic is kept while the equilibrium is not reached. For each wave reflection in the nozzle there is a reduction of the driver pressure.

The flow conditions in test section gradually change each time the expansion wave reflects at the nozzle entrance, consisting in the time that the wave expend to travel twice of the driver length, approximately. Because of these processes, is denoted that the test flow conditions change in a stepped manner and over the total operating time there are multiple test runs. Although just in the first one the set of test conditions is the aimed one. The high speed flow in the test section is sustained while the driver pressure is high enough. The operation processes are illustrated in Figure 3.14.

Figure 3.14 – Representation of the Ludwieg tube test run.

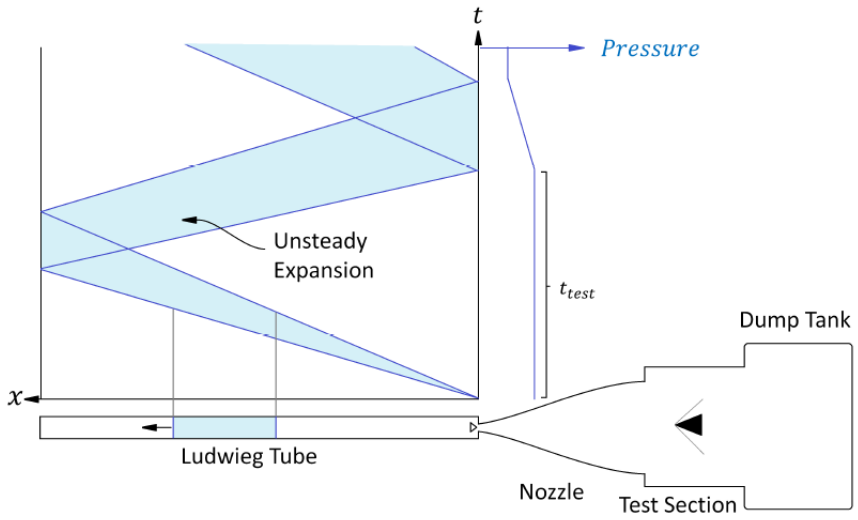

Source: Chung (2015).

The test time for a Ludwieg tube with continuous cross section area can be calculated by,

$$t = \frac{2L_{DT}}{c} \tag{3.2}$$

where L_{DT} is the length of driver and c the local speed of sound (KIMMEL et al., 2016). Of the total mass of gas stored, only a portion is properly consumed during the experiment, which is called test-slug. According to Çengel and Cimbala (2017), the local sound speed is simply calculated by

$$c = \sqrt{\gamma RT} \tag{3.3}$$

where γ is the ratio of specific heats for air, R is the gas constant and T the local static temperature. And, of course, the Mach number M is the adimensional that denotes how much times the flow velocity u is greater than c in a given position, thus $M = u/c$.

3.6.1 Governing Equations

3.6.1.1 Quasi-Unidimensional Isentropic Compressible Flow

The high speed flow in the Ludwieg tube after expansion in the nozzle can be considered as almost one-dimensional since the gradients parallel to the flow have the greatest magnitude compared to other directions. For Anderson (2003a), what differs the unidimensional from the quasi-unidimensional flow is that for the first case, the area of the cross

section of the fluid path is considered strictly constant. While for the quasi-unidimensional case, variations in the cross section are considered downstream the flow motion and the changes in the flow properties are consequence of the area change only.

The flow can still be treated as isentropic since that the generation of entropy in the real system occurs only in the boundary layer region close to the nozzle walls, corresponding to the edges of the fluid domain.

Still, considering that no shock waves are generated in the nozzle and disregarding friction, the behavior of the steady-state flow in the nozzle is in accordance with Euler's one-dimensional equations, from which the energy and continuity equations are obtained.

The expressions that describe the test flow in the Ludwieg tube are valid for isentropic flow, where isentropic processes holds for the majority of the fluid domain. This is defined in relation with two other thermodynamic concepts:

- **Adiabatic Process**: there is no heat exchange from the system to the external ambient.
- **Reversible Process**: dissipative effects don't take place: the effects of viscosity, thermal conductivity and mass diffusion are negligible.
- **Isentropic Process**: process that is both adiabatic and reversible.

The test section static conditions regarding pressure P, temperature T and density ρ are dependent to the accumulated driver stagnation conditions -P_0, T_0 and ρ_0,

$$\frac{T_0}{T} = 1 + \frac{\gamma - 1}{2} M^2 \tag{3.4}$$

$$\frac{P_0}{P} = \left(1 + \frac{\gamma - 1}{2} M^2\right)^{\frac{\gamma}{\gamma - 1}} \tag{3.5}$$

$$\frac{\rho_0}{\rho} = \left(1 + \frac{\gamma - 1}{2} M^2\right)^{\frac{1}{\gamma - 1}} \tag{3.6}$$

posterior to the passage of the expansion wave, the Mach number M and γ. Through this work, the test gas is treated as a perfect gas, thus $\gamma = 1.4$ and $R = 287 J/kg.K$ (ANDERSON, 2003a). The calculation of these conditions is further explained in the following sections.

3.6.1.2 Isentropic Flow with Area Change

Before applying the isentropic flow relations it is necessary to know the resultant Mach number after the nozzle expansion. As exposed in Anderson (2003a), the properties

of a ducted isentropic compressible flow can be altered due to area changes, following:

$$\frac{du}{u} = \frac{1}{(M^2-1)}\frac{dA}{A} \tag{3.7}$$

$$\frac{dP}{\rho u^2} = \frac{1}{(M^2-1)}\frac{dA}{A} \tag{3.8}$$

$$\frac{d\rho}{\rho} = -M^2\frac{du}{u} \tag{3.9}$$

The set of equations denotes the asymmetrical behaviour in the flow properties for subsonic and supersonic values of Mach number for narrowing and enlargement area changes. Finding the density/velocity ratio by isolating M^2 in 3.9 explains this change behaviour due to the conservation of the mass flow rate. For subsonic flows the density dilation is going to be less than velocity dilatation, so the velocity changes will be dominant among the compressibility effects. Then, the reduction of area causes the increase in velocity in order to maintain the flow rate. While for supersonic flows the opposite happens, and an area decrease causes the velocity to drop (ANDERSON, 2003b).

$$\begin{cases} M < 1 & \left|\frac{d\rho}{\rho}\right| < \left|\frac{du}{u}\right| \\ \\ M > 1 & \left|\frac{d\rho}{\rho}\right| > \left|\frac{du}{u}\right| \end{cases} \tag{3.10}$$

3.6.1.3 Area-Mach Relation

The previous analysis explain the utilization of a convergent-divergent nozzle, or Laval nozzle, to accelerate the stagnated gas to the desired Mach at the nozzle exit. The Area-Mach Relation as given by,

$$\left(\frac{A}{A^*}\right)^2 = \frac{1}{M^2}\left[\frac{2}{\gamma+1}\left(1+\frac{\gamma-1}{2}M^2\right)\right]^{(\gamma+1)/(\gamma-1)} \tag{3.11}$$

relates M and γ at any location of the nozzle according to the ratio of the local area A and nozzle throat area $A*$, where the flow is sonic. There are two possible solutions for every $A/A*$ in relation with the subsonic and supersonic nozzle sections.

3.6.1.4 Energy Equation

The Energy Equation provides the measure of the total energy of the flow, which for the facility operation is stored in the form of internal and kinetic energy (ÇENGEL; CIMBALA, 2017),

$$h_0 = h + \frac{u^2}{2} = constant \tag{3.12}$$

where the internal energy of the gas is measured by the enthalpy term h. Since the isentropic assumption holds for the majority of the domain, the total energy given by the stagnation enthalpy h_0 is constant. Following the isentropic assumption, it can be related to 3.4 (Caltech, 2014) as

$$\frac{h_0}{h} = \frac{T_0}{T} \tag{3.13}$$

where h can be further rewritten as:

$$h = \frac{u^2}{2\left(\frac{T_0}{T} - 1\right)} \tag{3.14}$$

Knowing the facility's enthalpy is relevant since it provides additional information for which types of experiments can be conducted. However, since h is mainly dependent on temperature and M, the values obtained for the Ludwieg shall be less than other pulsed facilities since the test flow is usually cold.

3.6.1.5 Initial Driver Tube Conditions

Due to the presence of the reflected shock wave inside the driver tube, the test gas initial conditions are different to the pre-run driver conditions before the valve opening. For this reason, it is useful to develop an analysis to predict the post-expansion gas conditions in order verify the experimental data collected during the test time (KIMMEL et al., 2016).

The equations for predicting the driver tube conditions behind the shock wave are followed if the continuity is satisfied by the driver Mach number, in other words, if the driver diameter is well designed to avoid the expansion wave reflection in any point except at the driver extremities. The post-expansion Mach number and γ determine the other flow properties as most of the relations are acquired from the isentropic flow expressions. Here, the subscript " DT " denotes the driver post-expansion conditions behind the shock wave, " i " denotes the driver pre-run conditions and " 0 " the driver stagnation conditions which will supply the test section flow conditions.

The Mach number is given by the area relation between the driver section and the

nozzle throat, eq. 3.15 (KIMMEL et al., 2016).

$$\left(\frac{A_{DT}}{A^*}\right)^2 = \frac{1}{M_{DT}^2}\left[\frac{2}{\gamma+1}\left(1+\frac{\gamma-1}{2}M_{DT}^2\right)\right]^{(\gamma+1)/(\gamma-1)} \tag{3.15}$$

The flow speed is related with the sound speeds, eq. 3.16.

$$u_{DT} = \frac{2}{\gamma-1}(c_i - c_{DT}) \tag{3.16}$$

The temperature ratios are given by eqs. 3.17,3.18,3.19.

$$\frac{T_i}{T_{DT}} = \left(1+\frac{\gamma-1}{2}M_{DT}\right)^2 \tag{3.17}$$

$$\frac{T_0}{T_{DT}} = 1+\frac{\gamma-1}{2}M_{DT}^2 \tag{3.18}$$

$$\frac{T_0}{T_i} = \frac{1+\frac{\gamma-1}{2}M_{DT}^2}{\left(1+\frac{\gamma-1}{2}M_{DT}\right)^2} \tag{3.19}$$

Finally, the pressure and density ratios are given in eq. 3.20.

$$\frac{P_0}{P_i} = \left(\frac{\rho_0}{\rho_i}\right)^{\gamma} = \left(\frac{T_0}{T_i}\right)^{\gamma/(\gamma-1)} \tag{3.20}$$

4 METHODOLOGY

The methodology that this project followed was based on a systems engineering approach. For that, a generic life cycle structure as described by INCOSE (2015), illustrated in Figure 4.1, was used as a primary model. Additionally, contributions from Pahl et al. (2005) and Romano (2003) will be used as a complement along the process. Referring to INCOSE (2015), this work will comprehend the phases of conceptual stage and partial development stage. The activities and objectives regarding each phase are explained in the following sections.

Figure 4.1 – Generic life cycle project.

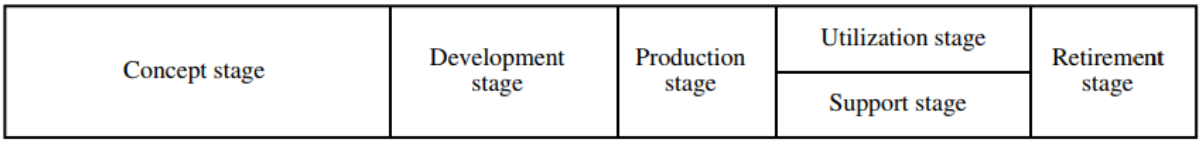

Source: INCOSE (2015).

4.1 CONCEPT STAGE

The kick-start of this initial stage is often driven by a demand: the identification of new organizational capabilities, opportunities or stakeholder needs. Then, the conceptual phase proceeds with an exploratory research to gather all relevant information and accumulate knowledge about possible candidates for the system of interest (SOI), while also studying new ideas and existent technologies. This research must be used to determine the potential technologies - and their issues - and identify what is feasible and what is not. Furthermore, the identification of technological risks and the technology readiness level (TRL) for each concepts is critical. These analyses will provide the insight needed to guide the selection of a SOI concept among the candidate systems analysed. Engineering models, mock-ups or other prototypes might be build and tested during this stage (INCOSE, 2015).

The research work executed during this stage is represented in this project as the the bibliography review of hypersonic wind tunnels presented along chapter 3, with the Ludwieg tube being the selected concept among the possible solutions.

Also during this stage the stakeholder needs are carefully reformulated to stakeholder requirements. According to Pahl et al. (2005) those requirements can be subdivided

into 3 distinct categories:

- **Basic Requirements:** understood as implicit requirements, they are not spoken by the stakeholder as are obvious functions that are expected that the SOI can perform.
- **Technical Requirements:** explicit requirements indicated by the stakeholder or confirmed upon feedback.
- **Attractive Requirements:** treated as implicit requirements, can lead to important differentials to the SOI designed.

After that, the requirements are valuated and will pass through a ranking process to sort the priority level of each. This is done to ensure that the SOI will indeed keep his top-level features and also prevent that too much time or budget are spent with the accomplishment of low priority requirements (ROMANO, 2003).

Finally, the main output from the conceptual stage are a SOI concept, better understanding of the stakeholder needs and formulation of the subsequent requirements, TRL assessment and rough estimate of cost and schedule.

4.2 DEVELOPMENT STAGE

During this stage, the stakeholder requirements are transformed into project requirements , which are described by engineering specifications. The activities are guided towards the main development stage goal: the definition and realization of the SOI that accomplish the stakeholder requirements and can be produced, utilized, supported and retired (INCOSE, 2015).

The development stage of this work is related to the analysis of the operation requirements for the Ludwieg tube and the mechanical project itself. This stage is partially completed along this project as the focus for this project is the preliminary definition of the main components of the facility.

5 RESULTS AND ANALYSIS

In this chapter are presented and discussed the main results obtained along each design phase according to the methodology adopted.

5.1 CONCEPT STAGE

As exposed by INCOSE (2015) the stakeholder needs are one of the drivers for the initial project research. Commonly the stakeholder, or clients, are external entities, organizations or individuals which will require a system of interest (SOI) to accomplish certain goals.

For the current work, however, the stakeholder needs are delivered by the author as the desired attributes for the SOI in the form of an hypersonic wind tunnel experimental facility. Those needs were formulated given the acknowledge of the author learned by the bibliography review from other works regarding Ludwieg tube facilities as well as the perception of the UFSM academic environment.

Among the existent pulsated facilities concepts, the Ludwieg tube concept was chosen by the features of this design that were acknowledged by the literature review presented in chapter 3.

The list of the stakeholder needs is presented on Table 5.1. The numeration does not denotes importance order for the needs.

Table 5.1 – Stakeholder needs.

N°	STK. NEED
1	Generate aprox. high-speed flight conditions
2	Safety
3	High research potential
4	Low-cost
5	Elevated durability

Source: Author.

The stakeholder needs were refined in order to attain the set of stakeholder requirements, presented on Table 5.2. The requirements types are classified as technical (T), basic (B) or attractive (A) (PAHL et al., 2005).

Table 5.2 – Stakeholder Requirements

N°	STK. NEED	N°	STK. REQUIREMENT	Type
1	Generate aprox. high-speed flight conditions	1	Sustain desired conditions at the test section	B
			Accumulate needed stagnation conditions at the driver section	
			Accelerate the test gas to the desired speed	
2	Safety	2	Guarantee the structural integrity of the facility	T
		3	Employ security systems to aliviate excessive internal pressure	T
		4	Monitoring of internal gas conditions	T
		5	Easy maintenance access	A
		6	Employ verified design codes and rules for the mechanical project	T
3	High research potential	7	Test section size with adequate dimensions	T
		8	Easy access to test section	A
		9	Long test time duration	T
		10	Multiple visualization windows at test section	T
		11	Multiple access ports and supports for data collection systems	T
		12	Good flow quality	T
		13	Generate both laminar, transient and turbulent flow regimes	T

Table 5.2 continued from previous page

N°	STK. NEED	N°	STK. REQUIREMENT	Type
4	Low-cost	14	Employ commercial components	T
		15	Reduce consumables needs for testing	A
		16	Low-cost operation	T
		17	Simple design and fabrication	A
		18	Simple assembly and installation	A
5	Elevated durabity	19	Corrosion resistance	T
		20	Long life-span	B
		21	Fatigue and creep resistance	T

Source: Author.

In the next step, the hierarchy of requirements is constructed by a valuation method (ROMANO, 2003). As described by Csillag (1995), all requirements are listed and applied into a Mudge Diagram. In this method, the requirements are compared in pairs for all possible combinations, in each "confrontation" the user decides which one possess a major importance and attribute the relative importance level by using weights associated to values on an ascending numeric scale. The total sum achieved by each individual requirement when compared to the remain defines the total importance level and will set the global rank for each requirement. Also, the percentage of the sum value comparatively with the global sum characterizes the relative importance level.

For this work, three levels of importance will be used. The weights and their associated values are set as follow: A = 5, B = 3 and C = 1. The Mudge Diagram built is presented in Appendix A.

Initially, need 1 was divided on 3 separate requirements, however it was difficult to set a importance order for the requirements since they directly dictate the generation of desired test flow conditions. They are all equally needed to characterize the test flow, as well as the test section conditions are a consequence from the stagnation and Mach number parameters. This way, they were all grouped into the same requirement.

The valuation results in A shows a balance between requirements from needs 1,2 and 5 mostly - comprised on the top 6 requirements group, but also including the flow quality requirement from need 3. The conservative approach adopted, giving priority for safe operation, is justified since the facility accumulates gas at high pressure and temperature conditions that can lead to serious injuries in cause of leakage or failure. This approach also originated a tie in the 4th and 6th priorities, between compromises of safety and flow quality and durability issues, respectively. As a side note, because of the first tie the next

position was moved directly to the 6th place, jumping the 5th position. This is a result from the native ranking function on Excel, however it does not interfere the ranking order neither the analysis.

5.2 DEVELOPMENT STAGE

The stakeholder requirements are further translated into project requirements (project metrics), capable to be quantitatively evaluated. The ranked list is shown on Table 5.3. All the ties previously seen in the Mudge Diagram are solved using the "duel" result from both requirements, prioritizing the winning one. The formulation of the operation requirements and mechanical project characteristics in the following sections are conceived to satisfy the stakeholder requirements according to their importance level and evaluated by the respective metrics.

Table 5.3 – Project Requirements

Rank	**STK. REQS.**	**PROJECT REQS.**	
1°	Guarantee the structural integrity of the facility	ASME Design Rules	Safety Factor (S.F.)
2°	Sustain desired conditions at the test section	Reynolds number	P (kPa), T (K)
	Accumulate needed stagnation conditions at the driver section	P_0 (MPa)	T_0 (K)
	Accelerate the test gas to the desired speed	Mach number	
3°	Facility and equipment long life-span	Service life (years)	
4°	Employ security systems to aliviate excessive internal pressure	Number of components (quantity)	
5°	Good flow quality	M_{DT}	Nozzle contour
6°	Corrosion resistance	Materials properties	
7°	Fatigue and creep resistance	ASME Design Rules	
8°	Test section size with adequate dimensions	Geometry (m)	
9°	Generate both laminar, transient and turbulent flow regimes	Reynolds number	

Table 5.3 continued from previous page

Rank	STK. REQS.	PROJECT REQS.	
10°	Low-cost operation	Cost of operation ($$)	
11°	Monitoring of internal gas conditions	Number of components (quantity)	
12°	Long test time duration	test time (s)	
13°	Multiple visualization windows at test section	Number of windows (quantity)	
14°	Easy access to test section	Geometry (m)	
15°	Employ commercial components	Number of components (quantity)	
16°	Multiple access ports and supports for data collection systems	Number of components (quantity)	
17°	Easy maintenance access	Geometry (m)	
18°	Reduce consumables needs for testing	Quantity of consumables	
19°	Simple design and fabrication	Number of commercial components (quantity)	
20°	Simple assembly and installation	Number of components (quantity)	Geometry (m)
21°	Employ verified design codes and rules for the mechanical project	ASME Design Rules	

Source: Author.

5.2.1 Operation Requirements

This section explains the methodology adopted to quantify the operation requirements of the Ludwieg tube which will impact in the mechanical project of the facility. The operational specifications are determined through the following analyzes:

- Generation of approximate high-speed flight conditions.
- Reynolds number and Mach number Similarity.
- Driver tube Mach number.

Through the studies, the isentropic relations were considered and the air was treated as a perfect gas. However, before demonstrating each analysis in greater detail, first the atmospheric flight conditions where high-speed flight takes place must be characterized.

5.2.1.1 High-Speed Flight Conditions

The surface heating of supersonic and hypersonic vehicles caused by air friction is extreme and represents one of the most challenging aspects on the development of this technology as higher it is the flight Mach number. To minimize this effect and avoid the disintegration of the vehicle, the hypersonic flight takes place on high altitudes where pressure and, especially, density of the atmospheric air is lower. Thus, the dynamic pressure loads can be alleviated (HICKS, 1993). Specially the altitudes situated on the stratosphere atmospheric layer corresponds to the region commonly used for experimental hypersonic and supersonic vehicles testing.

As these prototypes are propelled by air-breathing engines such as ramjet or scramjet, they cannot generate static thrust by its own and must be delivered by other means, typically by rocket propulsion, to be deployed with enough speed and in the desired altitude (TORO et al., 2018).

An altitude range from 20 km to 50 km is considered in this analysis to measure the atmospheric air conditions. Within this range, specially the 30 km altitude is a common altitude flight path for experimental high-speed vehicles. The variations on pressure, temperature and density with altitude are given according to the 1976 U.S. Standard Atmosphere (COESA) model (TEWARI, 2006), Figure 5.1. For some specific altitude levels the respective atmosphere conditions are summarized in Table 5.4.

Figure 5.1 – Atmospheric air conditions change with altitude.

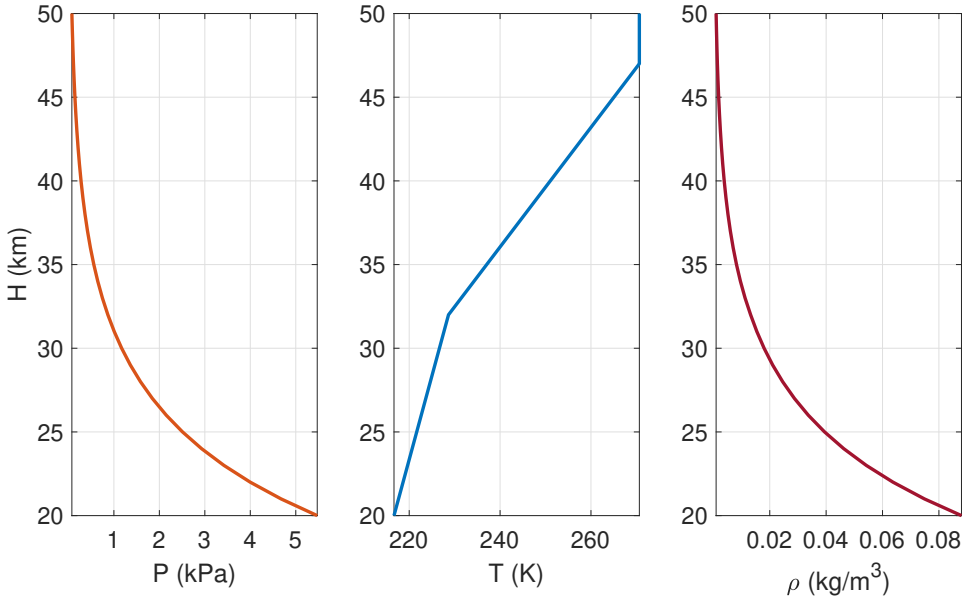

Source: Author.

Table 5.4 – Atmospheric air properties for specific altitude levels.

H (km)	P (kPa)	T (K)	ρ (kg/m^3)	c (m/s)
20	5.4722	216.65	0.088	295.04
25	2.5094	221.65	0.0394	298.4275
30	1.1710	226.65	0.018	301.7747
35	0.5584	237.05	0.0082	308.6206
40	0.2772	251.05	0.0038	317.6034
45	0.1430	265.05	0.0019	326.3389
50	0.0759	270.65	0.001	329.7684

Source: Author.

5.2.1.2 Reynolds number Similarity

To describe aerodynamic flow interactions, forces and moments acting upon the scale model in an analogous relation to the real vehicle, the Reynolds number similarity must be verified in both cases. The Mach number similarity is the second main parameter to be achieved in order to replicate the compressible phenomena of the fluid, i.e. shock waves behaviour.

This way, the facility operation requirements must be formulated to ensure a design Mach number with minimum deviation and the attainable Reynolds number range in the same magnitude order reached at atmospheric hypersonic flight. For that, the desired Reynolds number parameter must be comprised inside the operational Reynolds number envelope of the wind tunnel.

The Reynolds number is calculated by,

$$Re = \frac{\rho u L}{\mu} \tag{5.1}$$

according to Çengel and Cimbala (2017), where L is a reference length. As a common practice seen to generalize the analysis for wind tunnels, the reference length variable is dismissed in the calculation, resulting in a unit Reynolds number (1/m).

The dynamic viscosity μ for air at given temperature T is obtained by the Sutherland Correlation,

$$\mu = \mu_{ref} \left(\frac{T_{ref} + C}{T + C} \right) \left(\frac{T}{T_{ref}} \right)^{3/2} \tag{5.2}$$

this expression is employed due to the low static temperature levels achieved post expansion, which do not are usually shown on tables. The reference temperature used was T_{ref} = 273.15 K, where the respective value of the dynamic viscosity is μ_{ref} = 1.729E-05 kg/m.s (ÇENGEL; CIMBALA, 2017). The constant of Sutherland used is C = 103.0826 K.

For Mach number 3, 5, 7 and 9, and applying Equations 5.1 and 5.2 as well as the data from Table 5.4, the resulting unit Reynolds number graph for the reference altitude H range is given in Figure 5.2.

Figure 5.2 – Unit Reynolds number and altitude plot for different flight Mach numbers.

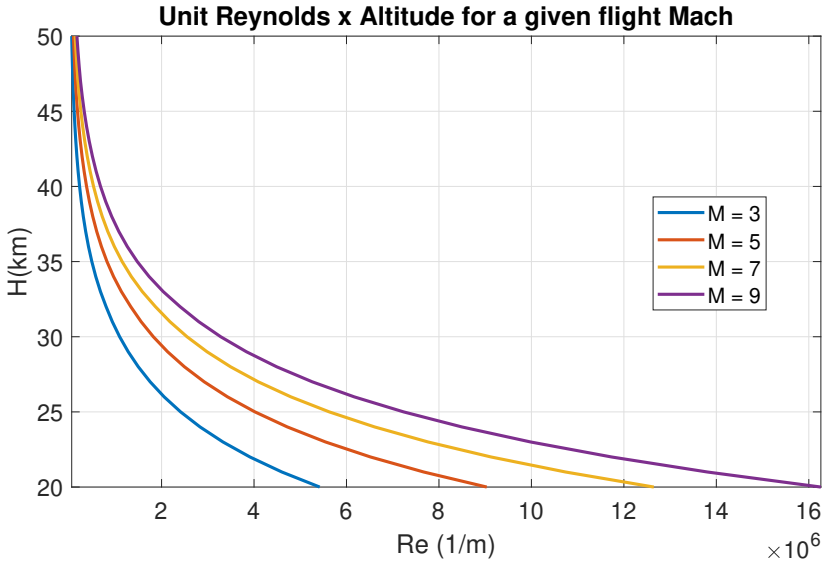

Source: Author.

The results demonstrate high magnitude order achieved by the Unit Reynolds mostly because the low viscosity and high flow velocity. However, as the density drop with the height increase becomes the dominant factor in the equation, also causing Reynolds to drop.

It is important to emphasize that the replication of the exact same flight conditions over a reduced model does not guarantee the flow similarity over the real size body. However, for testing of small components or other types of aerothermodynamics research, the capacity to generate approximate flight conditions, referring to pressure and temperature, is also relevant. So, some of the project requirements are also formulated to accomplish the operational capacity, which are discussed in more detail in the next section.

5.2.1.3 Driver Tube Stagnation Conditions

The driver tube initial conditions must be controlled mostly in order to attain the Reynolds number similarity for a given model. However, an analysis was also conducted to quantify the stagnation conditions requirements needed to generate exactly the set of flight conditions from Table 5.4, but now stretched to the 20-35 km range - which is more realistic for the current existent high-speed vehicles. This would give the capability to use 1:1 scale components, assuming that they could fit inside the test section. The isentropic flow relations from Equations 3.5 and 3.4 were used to this mean.

The stagnation pressure plot in the logarithmic scale in the vertical axis is shown below in Figure 5.3. For Mach number 5 and below the requirements on pressure dont't exceed 3 MPa for all the altitude ranges, which can be easily attainable on laboratory. For higher Mach numbers however, the P_0 condition increases exponentially. Usually, the Mach number independence principle can be applied in some cases to mitigate the some of the pre-run conditions (KLICHE; MUNDT; HIRSCHEL, 2011).

The stagnation temperature requirements are more extreme if compared with pressure, as shown by Figure 5.4 - vertical axis in logarithmic scale. Still for supersonic flight regime the T_0 prerequisite is around 1000 K near Mach number 4. While a free-piston compression system can provide the desired T_0, the electric heating employed in the Ludwieg tubes studied can generate a maximum attainable T_0 around 900 K. Most of the Ludwieg tubes with electrical heating operate with cold test flows. The heating is most used to avoid air condensation and freezing. But still, according to Radespiel et al. (2016), these cold gas facilities can be used for a wide range of fundamental research on hypersonics.

Figure 5.3 – Stagnation pressure requirements to replicate the exact real flight pressure conditions.

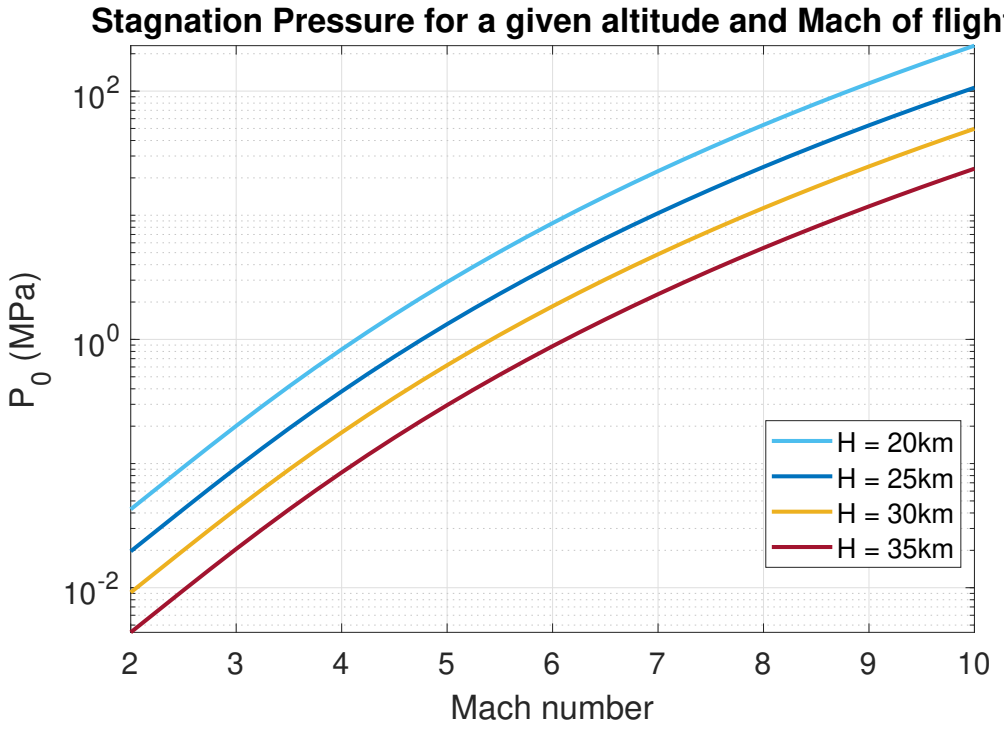

(a) Global P_0 requirements

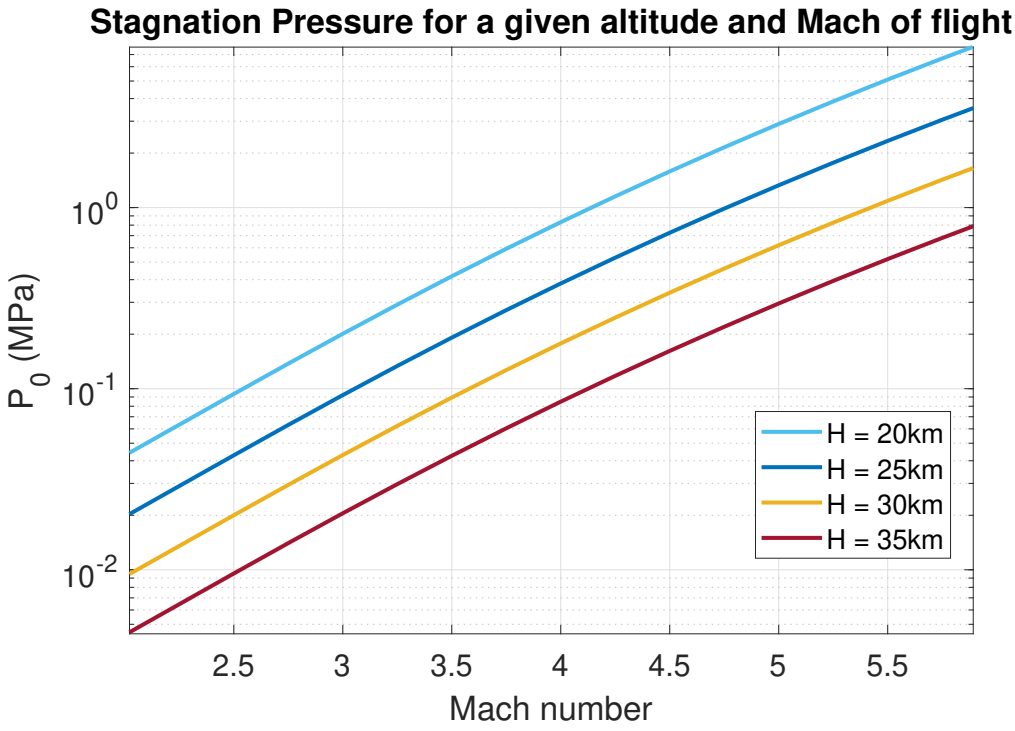

(b) Zoomed plot for supersonic and low hypersonic Mach number region.

Source: Author.

Figure 5.4 – Stagnation temperature requirements to replicate the exact real flight temperature conditions.

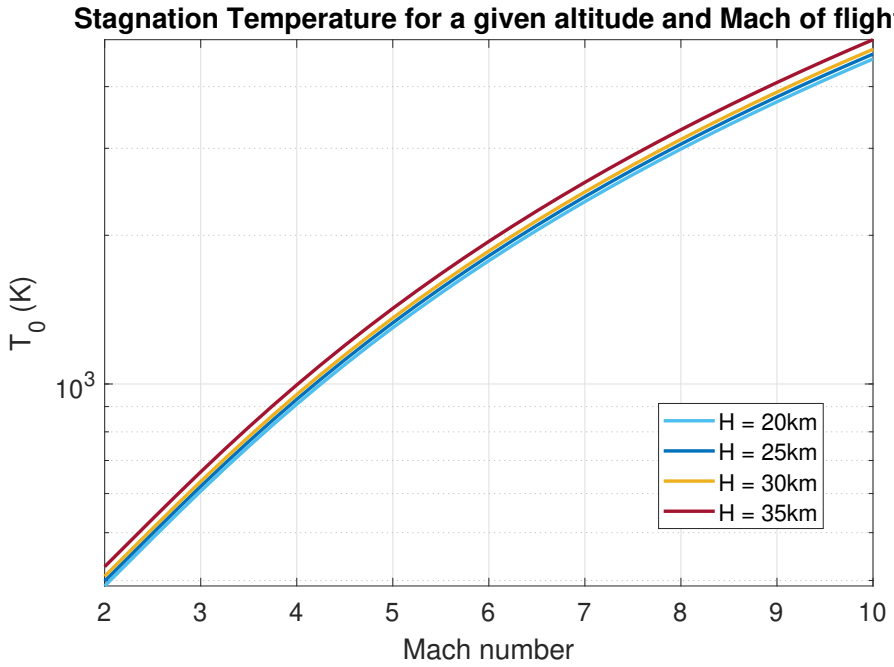

Source: Author.

5.2.1.4 Driver Tube Mach number

For each type of pulsed hypersonic facilities there are two primary requirements that must be ensured by the designed driver tube:

- The driver tube Mach number should be low enough ($M_{DT} < 0.05$) to ensure both good flow quality and approximated stagnation conditions.
- The driver should have enough gas storage volume to supply the facility operation timespan.

The insight on those parameters were given during e-mail exchange with the graduate student Eugene Hoffman who was involved with the design and construction of the UTSA Mach 7 Ludwieg tube along with Dr. Christopher Combs. Also, Radespiel et al. (2016) provides accordance with the M_{DT} restriction.

As given by Equation 3.15, M_{DT} is correlated with the area relation between driver and nozzle cross-sections. Also, as the nozzle is actually designed to be coupled into the test section, the driver internal area is linked to the test section size, which is one of the main input requirements for the mechanical project. In this regard, some analysis were made in order to evaluate the driver tube internal diameter (d_0) needed to satisfy different

requirements. For all analysis performed the test section was considered with a circular shape of internal diameter $d_3 = 0.5m$ while the axisymmetric isentropic nozzle exit diameter d_2 is set as $0.6d_3$. The stagnation temperature used is 750K and considered uniform in the driver tube.

The first analysis conducted was focused on quantify d_0 necessary to lock on required values of M_{DT} for a range of flight Mach numbers. The maximum value for M_{DT} considered is 0.084, which is the operational Mach value attained in the AFRL Ludwieg Tube (KIMMEL et al., 2016). The results are shown in Figure 5.5.

Figure 5.5 – Design of d_0 for different M_{DT} requirements.

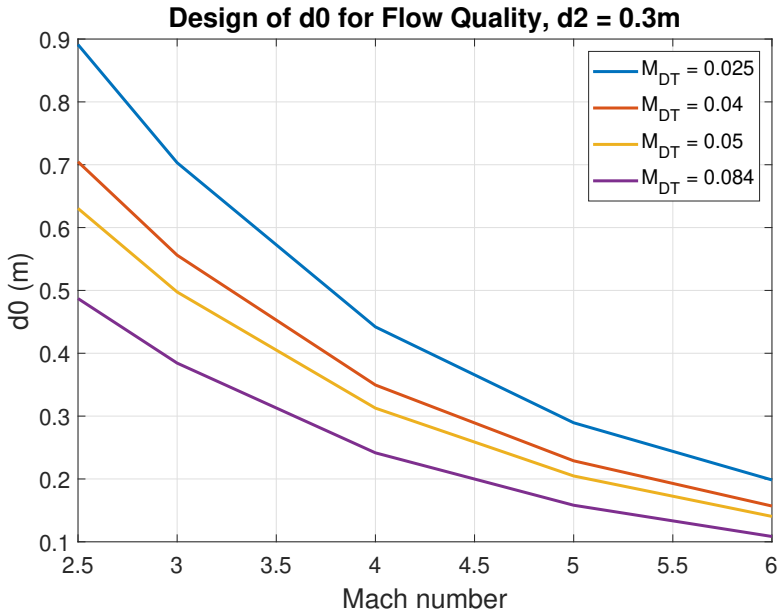

Source: Author.

This study illustrates the increase required in d_0 to lower M_{DT} for the same flight Mach number, as well as another considerable increase in d_0 as the M_{DT} plots approach lower Mach number values. This behaviour provides an important insight: even when the stagnation conditions requirements are less harsh for decreasing values of Mach, at the same time the growth of d_0 required to sustain a desired M_{DT}, without changing the test section dimensions, will difficult the feasibility of the mechanical project as well as increase costs, as pointed by Hoffman and Combs (2019).

In short, a Ludwieg tube designed under given key parameters - test section size, design operational Mach number, maximum stagnation conditions, the attainable experiments for a range of Mach number values, the lower and higher M limits will be limited in different ways. Considering nozzle replacements, the limitation for higher Mach numbers will be associate with the capacity of the laboratory equipment's to provide the stagnation conditions requirements and the safety factor associated to the mechanical integrity of the components when those conditions rise, especially at the driver section. While for lower

Mach numbers the limitation is linked to the degradation of the flow quality due to M_{DT} rise.

To quantify the performance of a facility outside the design Mach number, specifically for lower Mach number values inside the supersonic regime, another analysis was made. Using the results achieved on Figure 5.5, different driver configurations regarding d_0 and the resulting M_{DT} = [0.025, 0.04] were set for the same design Mach (M = 5). The results are illustrated in Figures 5.6 and 5.7.

Figure 5.6 – Analysis of flow quality for M_{DT} = 0.025.

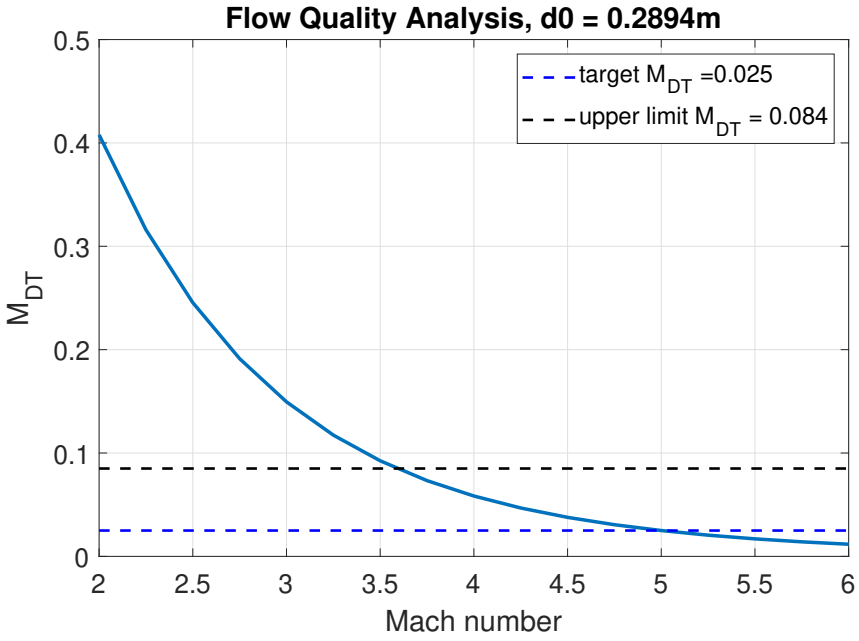

Source: Author.

Figure 5.7 – Analysis of flow quality for M_{DT} = 0.04.

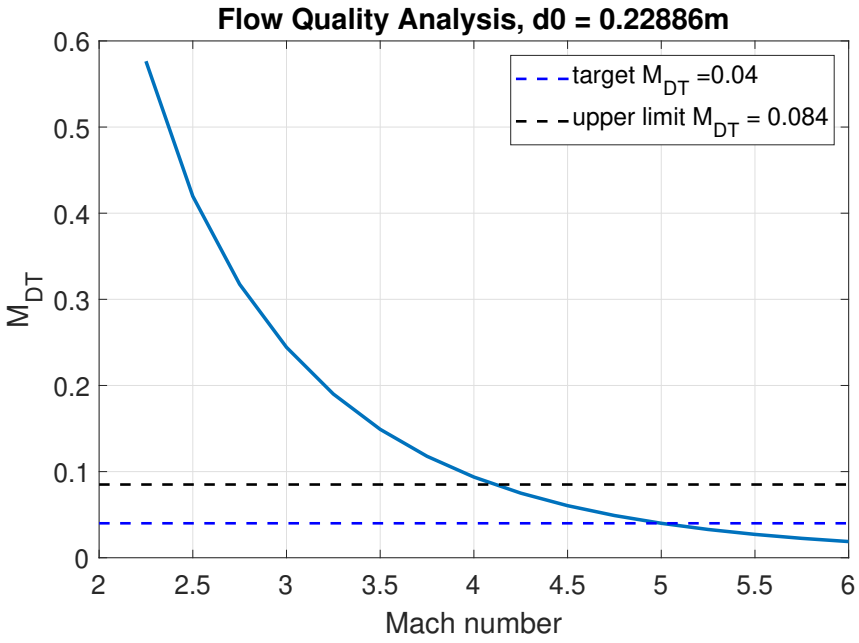

Source: Author.

Ensuring M_{DT} as low as 0.025 at Mach 5, Figure 5.6, in theory suggests that the Ludwieg tube could operate properly until near Mach 3.5, resulting in a considerable Mach range for experimental research. However, a great pipe cross-section area is needed for that. Rising M_{DT} to 0.04, Figure 5.7, the Mach range drops until near Mach 4, but the d_0 requirement is attenuated. Further analyzing Figure 5.7, a discontinuity occurs near Mach 2 as A^* becomes greater than A_{DT}.

The design choice for setting d_0 can be seen as a trade-off between conceivability and versatility of the facility. The first parameter can be benefited while maintaining high-quality flow levels and a wider Mach range by reducing the test section scale and consequently all the mechanical components upstream. However, this choice will impact the experimental data acquisition in the wind tunnel. Naturally, the test size reduction will diminish both core flow area and model size. As a consequence of that, less volume will be available for the installation of the experimental instrumentation. Else, smaller instrumentation components will be more expensive. However, theoretically although a wider attainable Mach range expands the versatility, many of the facilities seen in practice are used for flow characterisation studies focused on their respective design Mach numbers, given the extensive area that is the experimental research oh high-speed flows. In this manner, the benefits of a proper sized test section are more useful, with M_{DT} set around 0.04 to enhance flow quality.

A third analysis was made to verify the expected deviation on the initial driver conditions from the pre-run conditions, caused by the intensity of the expansion wave passage as a function of M_{DT}. This analysis indicate the offset needed in the pre-run conditions to start

the test run with the desired reservoir conditions. For that, equations 3.19 and 3.20 were implemented for M_{DT} values comprised between 0.025 and 0.125. Horizontal control lines were added for $M_{DT} = 0.04$ and $M_{DT} = 0.084$, comprising a zone with affordable values. The results are shown in Figure 5.8.

The calculated values of T_0/T_i and P_0/P_i along the interest region denotes small variations between the calibrated pre-run conditions and the stagnation conditions that will supply the hypersonic flow through the test run. As expected, the difference increases proportionally with M_{DT} as the gas converts more internal energy in form of speed. Pressure losses are seen to be more affected. The calculated values along the region are presented on Table 5.5.

Figure 5.8 – Analysis of stagnation conditions drop on test start.

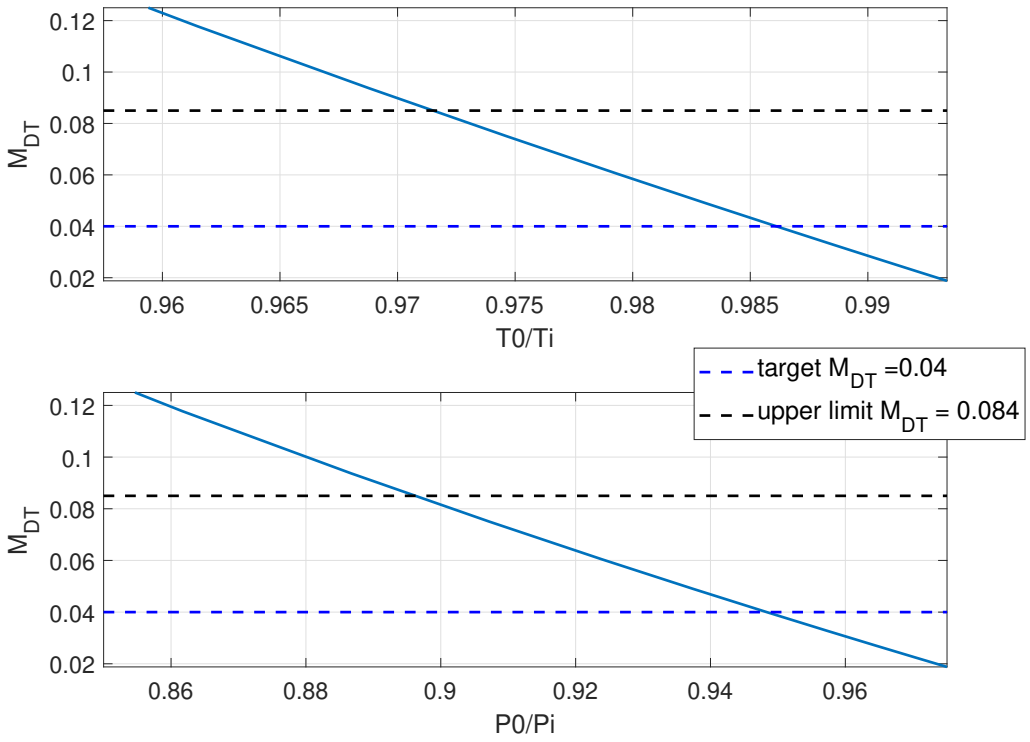

Source: Author.

Table 5.5 – Temperature and pressure losses.

M_{DT}	P_0/P_i	T_0/T_i
0.025	0.9671	0.9912
0.04	0.9483	0.9861
0.045	0.9422	0.9844
0.05	0.9362	0.9828
0.07	0.9129	0.9762
0.084	0.8972	0.9718

Source: Author.

5.2.2 Mechanical Project

This section presents the preliminary sizing an mechanical design of the following components for the proposed Ludwieg tube: driver section, test section and dump tank. Next, the main design choices, requirements and assumptions that will guide the proposed mechanical project are presented and discussed.

5.2.2.1 Key Parameters of the Facility

The Ludwieg tube of this project was chosen to be developed at the operational design point of Mach number 5. One of the criteria for this choice is related with the current capacity of the pulsed wind tunnels in Brazil. The shock tunnels present at IEAv are operated from intermediate to high hypersonic ranges - Mach 6 to 25 (TORO et al., 2008). So, a lower Mach number was chosen with the purpose to cover a different flow regime which is not being studied by experimental research due to the limitations of the shock tunnels itself. In this way, helping to diversify the scientific research. Else, for Mach number 5 the stagnation pressure requirements can be easily attainable in laboratory and the flow quality can be achieved without the expense of a large driver tube diameter.

A 500 mm cross-section size test chamber is considered very suitable for fundamental research (RADESPIEL et al., 2016). It can provide enough space for test models - with a maximum model width of around l_{max} = 200 mm, and data acquisition devices, similar to the capacity of the USAFA Ludwieg tube (CUMMINGS; MCLAUGHLIN, 2012). The test time is desired to be set around t = 100 ms to afford a wider variety of data acquisition techniques and quantity of measurements for each test run. The driver Mach number is set on M_{DT}

= 0.045 to assure good flow quality. The stagnation temperature is expected to be as high as T_0 = 750 K, by analyzing the heating capacity achieved existent Ludwieg tube facilities by electric heating (KIMMEL et al., 2016; BASHOR; COMBS, 2019). For this initial phase of the facility's project the whole driver tube is considered to be heated, therefore having an uniform internal diameter. Also, this design choice can simplify the project as dismisses greater tubing parts for the non-heated section and also increment the research potential as it could be hypothetically used for other operational Mach numbers. Although the UTSA facility applies partial heating of an uniform driver without noticing any performance degradation (BASHOR et al., 2019) - while also reducing operation costs. But due to the size difference between this facility and the proposed one for this work, this effect might not be the same. This is another design aspect that will be considered in a more mature stage of this project, if necessary.

By the results obtained from the stagnation conditions requirements analysis (Figure 5.3), the maximum P_0 needed to generate approximate real flight conditions is roughly 3 MPa. However a safety factor was introduced to extended the maximum allowable pressure of the facility to 8 MPa, then an additional safety factor of $S.F$ = 2.67. This limit was imposed to both guarantee safe operation and widen the attainable Unit Reynolds envelope, estimated to range from Re = 5 x 10^6 m^{-1} to 50 x 10^6 m^{-1} by analyzing the capacity of existent facilities.

Finally, the complete set initial key parameters of the proposed facility are compiled in Table 5.6.

Table 5.6 – Proposed Ludwieg tube key parameters

Key Parameters	
M	5
d_3	500 mm
l_{max}	200 mm
t	100 ms
M_{DT}	0.045
P_{0max}	8 MPa
$S.F.$	2.67
T_{0max}	750 K

Source: Author.

5.2.2.2 Material Selection

The high temperature needed for the test slug in order to avoid condensation inside the test section limits the construction materials available for the driver tube (HOFFMAN; COMBS, 2019). Either the heating temperature exceeds the maximum service temperature of metallic alloys, such as for aluminium, or dramatically weakens the material's allowable stress $\sigma_{allow.}$ to withstand the pressure requirements. The variations of $\sigma_{allow.}$ with temperature for common metallic alloys used in wind tunnels is illustrated in Figure 5.9.

Figure 5.9 – Allowable stress plots for aluminium (AL), carbon steel (CS) and stainless steel grades (SS) according to temperature.

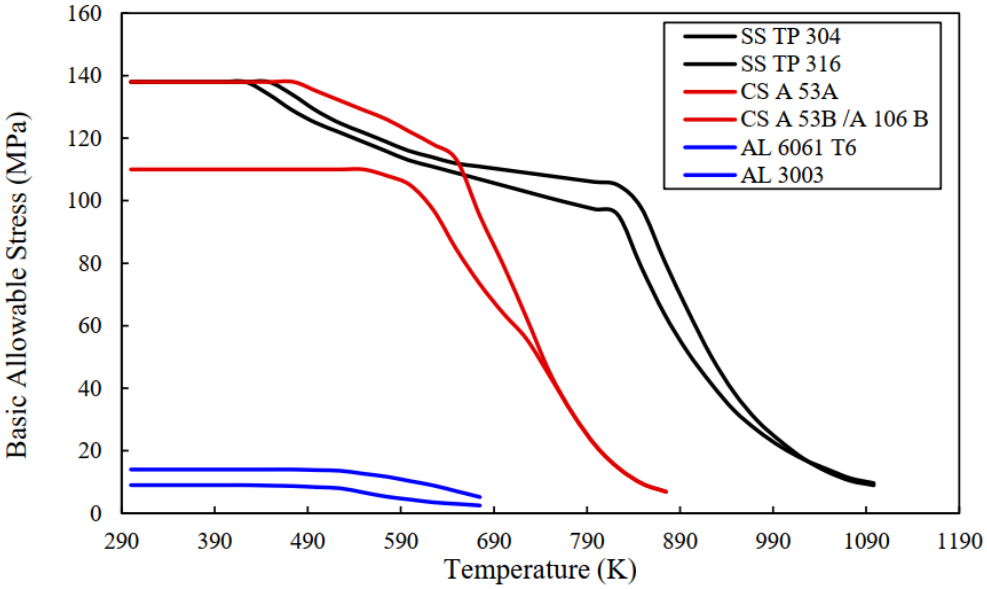

Source: Adapted from Hoffman and Combs (2019)

The stainless steel (SS), grade SA312 TP304, as given by ASME (2017) was chosen for the fabrication of the driver components. Similar stainless steel grades were seen to be commonly used in hypersonic wind tunnels, as presented by Kimmel et al. (2016), Cummings and Mclaughlin (2012) and others, due to its strength properties in high temperatures and excellent corrosion resistance, both factors which benefit the maintenance and lifespan of the facilities. The main disadvantage really is the high cost of the material when compared to more common pipping materials, such as carbon steel. In Figure 5.10 is shown the plot of σ_{allow} in respect of temperature for the material as listed in ASME (2017). The data tip illustrates the value of σ_{allow} = 74.7 MPa at $T0$ = 750 K that is used for the driver mechanical project. The allowable stress values established by ASME (2017) have a built-in safety factor of approximately 3.5. However in reason to the safe operation requirements it is desired to work at a maximum stress levels below this limit for the driver section.

Figure 5.10 – Allowable stress plot for steel grade SA312 TP304 according to temperature.

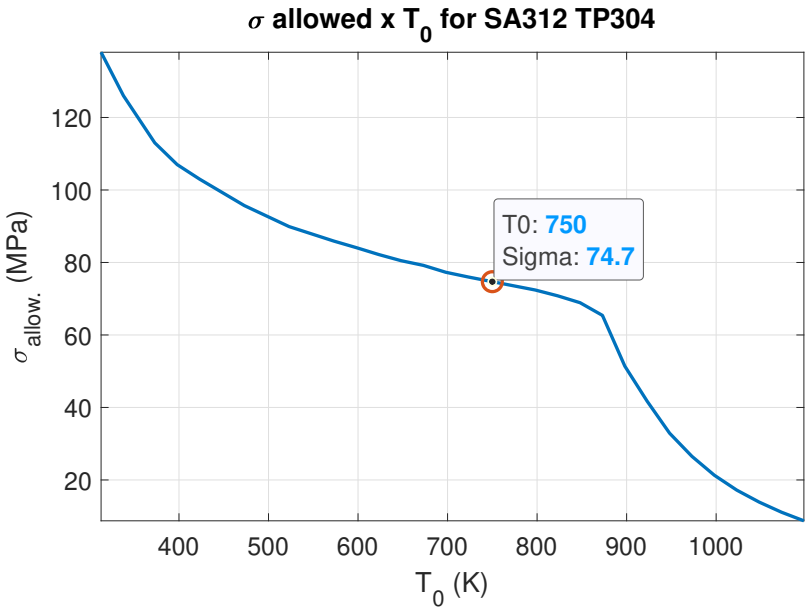

Source: Author.

5.2.2.3 Components Mechanical Project

- **Driver Tube**

A driver tube section capable to provide M_{DT} = 0.045 was chosen, corresponding to an internal diameter of d_0 = 215.8 mm (NPS 8). The tube components wall thickness was evaluated as e = 12.25 mm by Eq. 5.3 for straight pipe under internal pressure as described on ASME Code for Pressure Piping B31.3 (ASME, 2016). The internal mechanical tolerance b_i estimated is 0.5 mm and the remaining parameters of pressure and maximum allowable stress, as described previously, are P_0 = 8 MPa and σ_{allow} = 74.7 MPa at T_0 = 750 K.

$$e = \frac{d0 + 2b_i}{2}\left[exp\left(\frac{P_0}{\sigma_{allow}}\right) - 1\right] \tag{5.3}$$

To achieve a test time duration of 100 ms, the driver length required according to 3.2 is L_{DT} = 27 m, similar to the facility from Cummings and Mclaughlin (2012). A resulting hydraulic volume is evaluated in V_{DT} = 0.98 m^3. A folded driver approach is applied in order to reduce the total length of the apparatus (KIMMEL et al., 2016; SCHRIJER; BANNINK, 2010). For that, a 180° long radius return - as given by ASME B16.9 (ASME, 2001)- is

placed on the mid point of the driver tube length.

All of the driver tube mechanical characteristics described are summarized in Table 5.7.

Table 5.7 – Driver section main mechanical specifications.

Driver Specifications	
$d0$	215.8 mm
e	12.25 mm
L_{DT}	27 m
V_{DT}	0.98 m^3
Material	ASME A312 TP304

Source: Author.

The tube sections are interconnected by flange connections welded on the tubes extremities. For that, both endings are beveled for the welding fillet deposition. It is also expected to use stainless steel on the flange parts. For the given material, the flange class 900 is the most suitable for operating under the facility conditions according to ASME Code B16.5 (ASME, 2013). For this class and environment, a set of 12 stud bolts A193 B16 and 24 heavy hex nuts A194 2H and washers are required to fasten adjacent flanges facings. Additionally, the flange type weld-neck with ring-type joint facing is the preferred choice for the facility.

The ring-type joint (RTJ) facing flanges don't use regular flat gaskets for sealing, instead uses a round metallic ring fitted in a groove cut into the flange face. The ring creates a tight seal as the bolts tighten the assembly together with the internal gas pressure. Due to the enhanced sealing capacity, the RTJ facing is considered the most efficient in process piping systems (PARISHER; RHEA, 2012). According to ASME B16.20 (ASME, 2012), the ring joint gasket shall be made of a softer material than the mating flanges as they shall deform instead of the primary structures. In this case, a R49 soft iron or low carbon gasket could be used while supporting high temperatures.

Weld neck flanges provides higher strength and structural resistance as a benefit from the gradual thickness increase along the tapered hub. This design feature improves the reliability over operation conditions under piping thermal dilatation. Due to this characteristics, weld neck flanges are used in severe pressure and temperature service conditions. Finally, the hub hole diameter is chosen to match the piping internal diameter. Hence, the precise matching adjustment eliminates erosion and turbulence in the internal flow (PARISHER; RHEA, 2012). The flange connection assembly with the specifications mentioned is showed in Figure 5.11. All the parts can be found on market.

Plus, a blind flange class 900 is used for sealing the driver tube end. As described by Cummings and Mclaughlin (2012), this part can be machined for the insertion of the

pressure port where the driver tube is filled. According to Caltech (2014), near the driver end is one possible location for installation of a safety release valve.

Figure 5.11 – Flange connection assembly in exploded view.

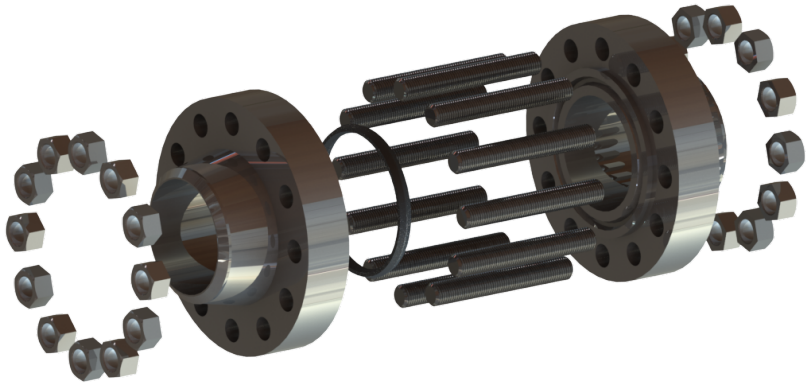

Source: Author.

The test gas is heated by an electrical resistance placed in the driver gas feeding system. Namely, a Sylvania SureHeat© MAX 18kW Heater, Figure 5.12 could provide the required output temperature. This exact same component is employed by the AFRL Ludwieg tube - which employs a similar driver tube internal diameter (NPS 9 driver section), to achieve the required stagnation temperature (KIMMEL et al., 2016). The filtered dry air flows through the resistance, however at a pressure lower than 400 kPa to not exceed the maximum air pressure of the device. Finally, the driver section shall be covered with an insulating material such as rock wool pipe shells to minimize heat loses and maintain the thermal comfort of the laboratory.

Figure 5.12 – Sylvania 18kW electrical air heater.

Source: CPIHEAT (2020).

Another aspect that shall be taken in account is the thermal dilatation of the com-

ponents. Other pulsed facilities like shock-tunnels and expansion tunnels can achieve very high temperatures, but for short amount of time. The period where the high temperatures are keep in a heated Ludwieg tube corresponds to the pre-run time which could vary between a couple minutes or even some hours according to the bibliography. This time could be sufficient for the volume pre-heated filled gas substantially increase the driver tubing parts temperature. The condition is more extreme for external heating devices such as as heating blankets and cables which directly transfer energy to the outside surface of the tubing sections. Unfortunately, this phenomena is not yet fully understood during this work.

Upon contact with the personnel from the UTSA facility, it was related that the heat generated by the heating tapes quickly dissipates, not trespassing much past the flanges and not affecting the remaining downstream sections. However the driver diameter of this facility is approximately 87 mm, with only partial heating. Again, this behaviour might not appear in the same way for the proposed facility.

Considering the great length of this section it is expected that the thermal dilatation can be expressive. One way to alleviate resulting structural stresses is providing space for these dilatations occur without restriction. One possible solution is the use of wheeled under-carriages, Figure 5.13, connected to the supports, as seen in the AFRL and USAFA wind-tunnels, (KIMMEL et al., 2016; CUMMINGS; MCLAUGHLIN, 2012). This design also allows better flexibility for moving the components, required for maintenance access or modifications.

Figure 5.13 – Movable under-carriage supports, seen at the extremes of the driver length and test section.

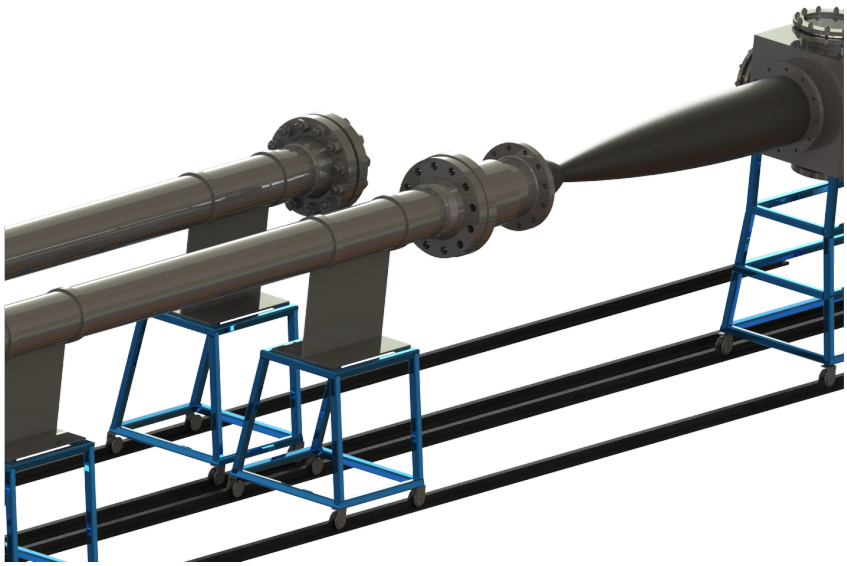

Source: Author.

- **Test-Run Triggering Component**

As described previously, the test-run triggering component can be diaphragms or a

fast action valve. The fast action valve benefits lower operation costs, agility between test runs, and most importantly: denies the use of consumables. The availability and acquisition of experimental material is one of the main issues for public academic research in Brazil. However, it was not found commercial models of this component. Consequently, it has to be designed from scratch with fitting specifications for the facility. As another SOI, the component will have their own life-cycle, development costs and a set of project requirements which will be distributed in part to the design of electronic and pneumatic components related to the valve concept.

The difficulties seen for the fast action valve implementation are mitigated by the use of diaphragms, which are cheap and can be easily integrated in the facility. The buffer configuration is preferred as it promotes a better rupture control. Martos (2014) and Toro et al. (2006) describe a double diaphragm section with a sleeve system used in the T3 shock-tunnel, Figure 5.14. The design provides easy access for diaphragm replacement while also avoiding moving the remaining sections for this task. Due to the trade-offs between both options it is desirable that the facility could be compatible with both concepts. But the proposed Ludwieg tube initially could operate with double diaphragms in a similar assembly as described.

Figure 5.14 – Sleeve assembly for the double diaphragm section.

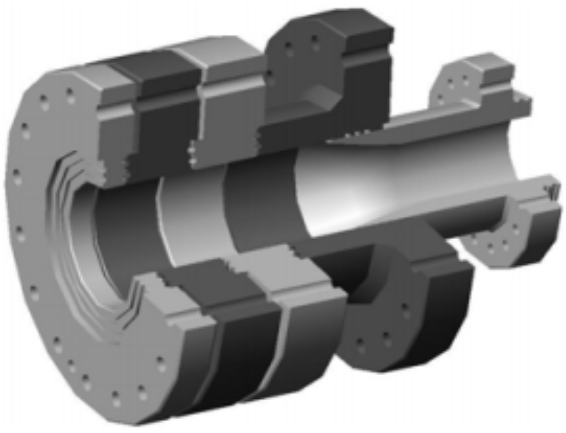

Source: Toro et al. (2006).

- **Nozzle**

The nozzle is the hearth of any pulsed wind tunnel, used to accelerate the flow to high-speeds and guarantee the flow quality inside the test section. The most simple design possible is a conical nozzle, however in general the flow presents an irregular distribution on the velocity profile at the exit area due to the inclination of the streamlines. This results in a poor flow quality that impacts the research potential of the facility.

It is imperative to generate good flow quality within the test section and the nozzle contour is fundamental for that. A De Laval nozzle designed with a feasible length and

counting the boundary layer growth might be developed with a MOC/BL method coupled with optimization to geometric constraints. A more refined geometry can also be attained with the method described by Chan et al. (2018) depending on the computing power available. The nozzle manufacture cost is usually high due to the precision needed to sculpt the wall contour.

Axisymmetric steel nozzles can be fabricated by machining process although produces a great amount of material waste. Larger components might be segmented into different parts to benefit the manufacture, as seen in Toro et al. (2006), however increasing the assembly complexity.

Alternatively, the state of art on additive manufacturing processes can produce large and complex 3D components as a single piece with verified reliability. The benefits also extend to the better performance and extended durability of the components, as well as faster production (SIEMENS, 2020). Although the surface roughness of the final product must be evaluated, as a higher roughness will directly alter the friction coefficient at the nozzle walls and the boundary layer interactions.

Finally, another possible fabrication method is through fiber-glass lamination. A 2m long fiber-glass composite nozzle is used for the USAFA facility, with metal bores on both extremities for flange mating. The final surface roughness is said to be minimal.

- **Test Section and Dump-Tank**

The test section will not face operation conditions as harsh as in the driver section. This way, the design is principally guided considering the ease of operation (operators access, internal volume, quantity and location of access windows, height from lab floor), setup for measurement techniques and access for instrumentation.

Three distinct concepts for the test section are suggested. The designs were chosen analyzing some operational facilities characteristics. But first, some key requirements were formulated which all the concepts must have. A circular 500mm diameter cross-section is set as one of the key parameters of the facility mentioned previously. The total length is estimated as 1 m and the height of the test section center-line from the lab floor is set to 1.3 m. The test section shall contain at least four circular windows distributed radially. An adequate diameter of 260 mm is estimated for the windows as detailed from the USAFA facility by Cummings and Mclaughlin (2012).

Welded flange-like structures can be used to insert the windows, with the assembly sealed with o-rings and fixed by bolted counter flanges. A pair of horizontal opposite windows shall be used for Schlieren imaging, where a light source must trespass the test flow from one aperture to another. A vertical upper window can be used for non-intrusive laser measuring technique. The last window is placed below the model and is used for passage of instruments wiring and cables. A similar layout is seen for the T3 according to Toro et al. (2008).

Meanwhile, the key parameter related to the dump tank is an estimated internal volume of roughly 14 m^3. Which was evaluated comparing V_{DT} from the USAFA and the one designed, 0.53 m^3 and 0.97 m^3 respectively.

The first concept is similar to the own T3 test section (TORO et al., 2006), but scaled down to the dimensions mentioned, Figure 5.15. The operators access to the test section can be through the windows or by entering inside the dump tank, which is directly mounted downstream the test section. There is no diffuser in this concept. This facility features a vertical dump of 4.5 m in height and 2 m in diameter. On Figure 5.16 the dump tank is illustrated along with a 1.75 m operator dummy. For the T3 facility, the dump tank was also designed to be trespassed by a long sting support used to sustain models into the test section with minimal interference from the support itself.

The second concept is derived from the USAFA Ludwieg tube by Cummings and Mclaughlin (2012). The test section is similar to the previous concept, but with a rectangular access at the bottom used as a probe chamber, which can comport a linear motion unit and a pitot rake, Figure 5.17. The main difference is that the internal access is done by sliding the 1m long diffuser section inside the dump-tank, which is mounted horizontally, Figure 5.18. For that, a set of roller guides are mounted near the dump tank entrance. Additionally, inflatable sealing rings in this region ensure the agreement to both sealing efficiency and diffuser sliding mechanism, firmly sealing the tube when pressurized but also allowing the diffuser movement when needed. It is believed that the access and work room is also improved in this case, however the additional mechanisms involved can increase costs and complexity. This design also introduces the installation of a model support between test section and diffuser flange connections.

Figure 5.15 – Test Section Concept 1.

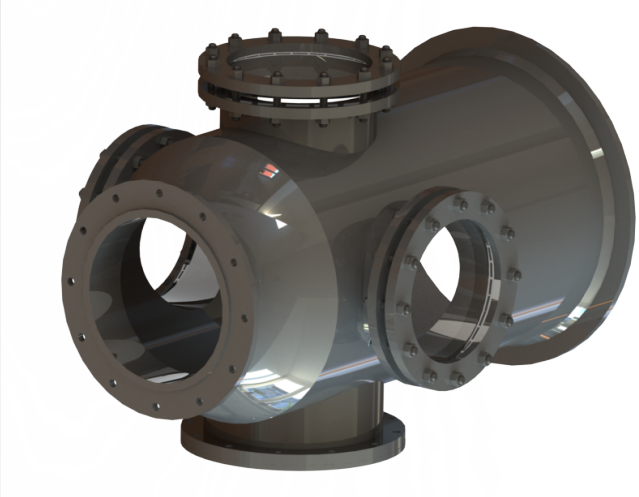

Source: Author.

Figure 5.16 – Dump Tank Concept 1.

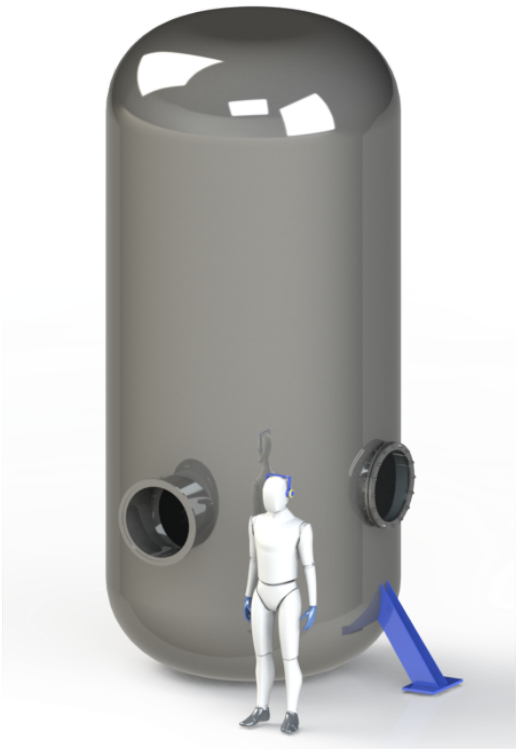

Source: Author.

Figure 5.17 – Test Section Concept 2.

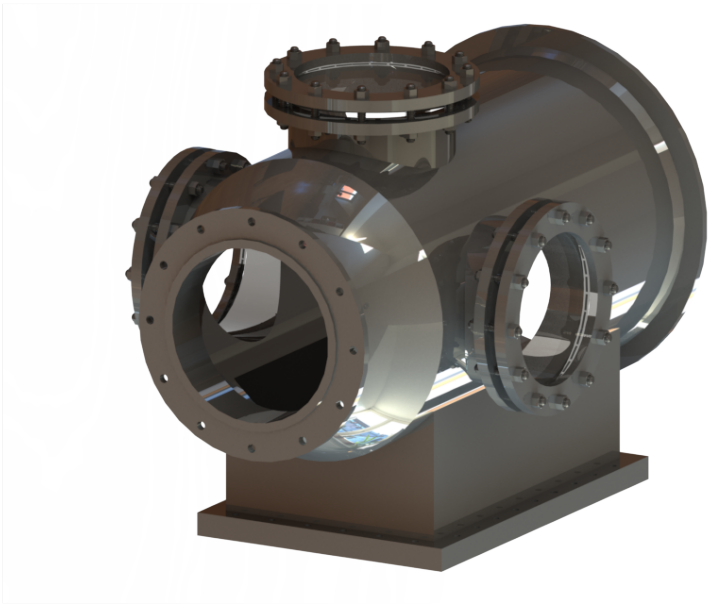

Source: Author.

Figure 5.18 – Dump Tank Concept 2.

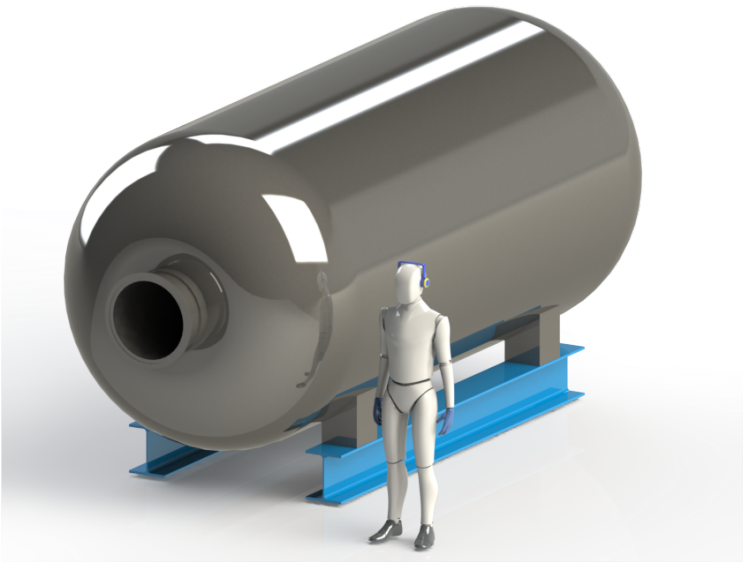

Source: Author.

Finally, the third test section concept is an adaptation of the square test section from the UTSA Ludwieg tube. Here, a lateral hinged door is used for internal access (BASHOR et al., 2019), Figure 5.19. This feature could provide a greater flexibility to access the interior for minor adjustments in comparison with the other methods described. However, the wall thickness would need to be greater in order to machine bolt holes for fixing the door on test runs. The desired windows display were then added on this design to satisfy the operational capabilities.

Figure 5.19 – Test Section Concept 3.

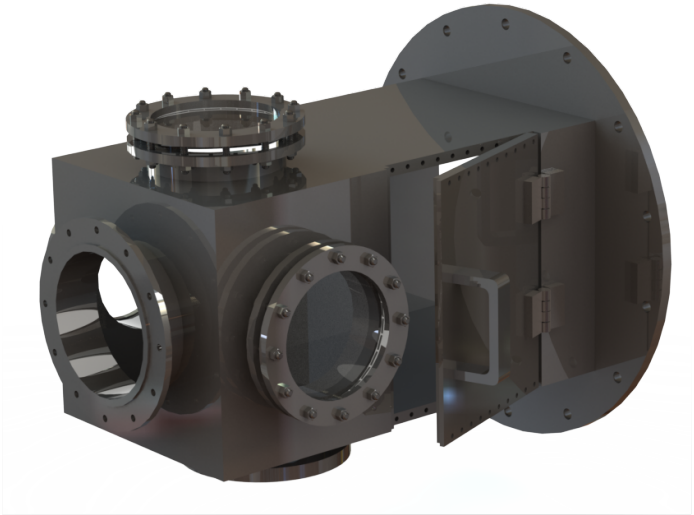

Source: Author.

Upon all the different concepts, the test section 3 could provide additional internal access facility. Comparing with the remaining concepts, the last one provides a differential in regard with REQS. 14 and 17. Requirement 16 can also be benefited with the installation of an additional small support fixed on the test section floor with direct access.

Additionally, if the test section component should be built from scratch, the box shape might be the best choice for budget as it could be built from flat welded steel sheets. But it depends from the manufacturer. In sum, considering possible benefits from the hinged door mechanism, it is the selected concept for the preliminary project.

The sliding diffuser tube seen for the dump tank concept 2 is also a desirable capacity for the same reason. It can provide easy access for model adjustments mounted on the diffuser. Given the large reservoir size dimensions, specially in radius, the mechanism original to concept 2 could be adapted for a vertical dump tank. The orientation choice relies on laboratory room size. For the present case, given the driver length, a vertical orientation is preferred to mitigate a little the total facility length.

Concluding, a 3D render of the proposed facility with the concepts chosen is presented in Appendix B.

5.2.3 Reynolds number Envelope

Using different sets of pre-run conditions within the allowable operational range it is possible to determine the operational Reynolds Envelope of the facility at the design Mach. This analysis provide insight upon the range of unit free-stream Reynolds number attainable which will characterize the flow regime experienced by scale models and other experiments.

The pressure range is taken at the lower value of 1 MPa to 6 MPa at max, below the maximum pressure of 8 MPa. The temperature range is set between 500 K and 750 K. The minimum T_0 value was also adopted for the operational envelope formulation of the USAFA Ludwieg tube. According to Cummings and Mclaughlin (2012), for lower stagnation temperatures near this value the test gas condensation is expected to occur. Finally, applying the flow conditions range into the set of isentropic governing equations as well as Equations 5.1 and 5.2 the Unit Reynolds envelope is obtained as illustrated in Figure 5.20.

As previously discussed, the test section hypersonic flow is cold and the enthalpy levels obtained are not as high comparatively to other pulsed facilities, measured in the MJ scale. Table 5.8 presents the temperature levels and their respective calculated dynamic viscosity as well as the resulting enthalpy levels evaluated using Equations 3.14 and 3.12.

Figure 5.20 – Operational Reynolds Envelope for the proposed Ludwieg tube.

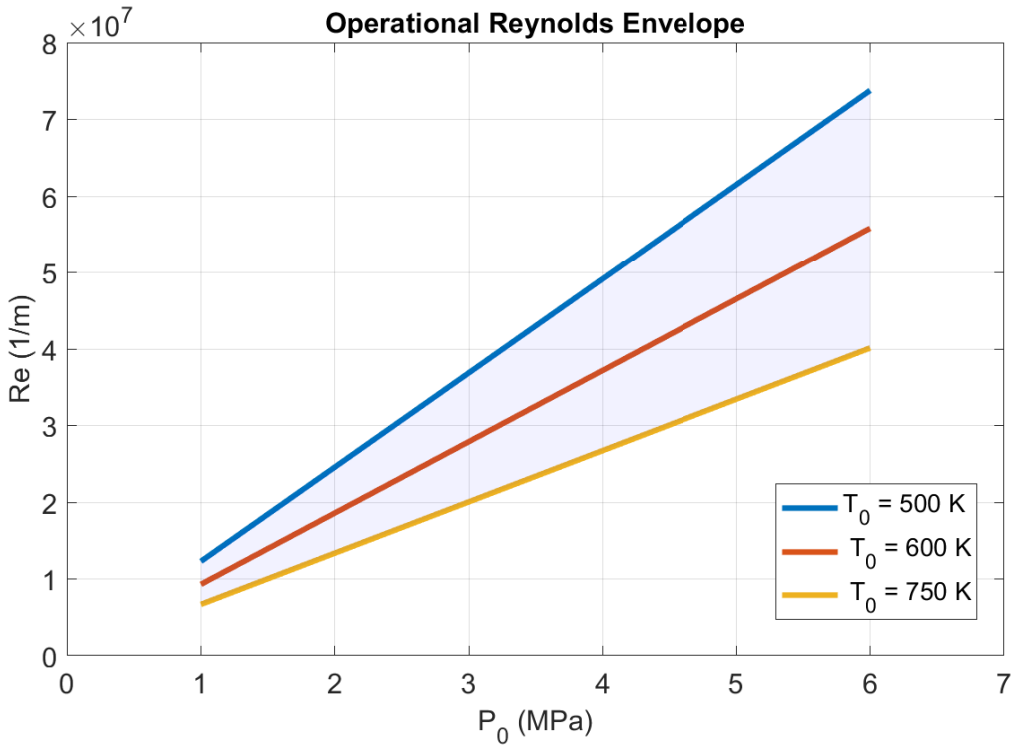

Source: Author.

Table 5.8 – Static temperatures, dynamic viscosity's and enthalpy levels for the attainable test section flows inside the Reynolds number Envelope.

T_0 (K)	T (K)	μ (kg/m.s)	h (kJ)	h_0 (kJ)
750	125	8.8292E-6	125.56	753.38
600	100	7.0954E-6	100.45	602.7
500	83.33	5.8802E-6	83.71	502.25

Source: Author.

The UFSM proposed facility could provide unit Reynolds ranging from 6.68 x 10^6 to 73.78 x 10^6. This interval comprises other facilities unit Reynolds capabilities, Table 5.9.

But most important, the facility is, in theory, capable to provide unit Reynolds in a higher magnitude order than those seen for real flight at Mach number 5, summarized from Figure 5.2 on Table 5.10. The Reynolds number similarity should be achieved with the proper adjustment of the test artifacts dimensions and the Ludwieg tube calibration.

Table 5.9 – Unit Reynolds range comparison with another Ludwieg tubes.

Name	**Mach number**	**Re (m^{-1})**
UTSI	4	48 x 10^6
AFRL	6	13 x 10^6 to 34 x 10^6
BAM6QT	6	11 x 10^6
USAFA	6	5 x 10^6 to 32.5 x 10^6
UTSA	7	47 x 10^6
UFSM	5	6.68 x 10^6 to 73.78 x 10^6

Source: (LINDORFER et al., 2016; BASHOR et al., 2019; CUMMINGS; MCLAUGHLIN, 2012; KIMMEL et al., 2016).

Table 5.10 – Unit Reynolds and dynamic viscosity for different altitude levels at Mach 5.

H (km)	**T (K)**	**u (m/s)**	**μ (kg/m.s)**	**Re (1/m)**
20	216.65	1.4752E3	0.1437E-4	9.0339E6
25	221.65	1.4921E3	0.1464E-4	4.0199E6
30	226.65	1.5089E3	0.1491E-4	1.8216E6
35	237.05	1.5431E3	0.1546E-4	0.8192E6
40	251.05	1.588E3	0.1619E-4	0.3775E6
45	265.05	1.6317E3	0.1689E-4	0.1816E6
50	270.65	1.6488E3	0.1717E-4	0.0938E6

Source: Author.

6 CONCLUSION

This work performed an initial approach on the development of a Mach number 5 Ludwieg tube. A set of 21 requirements were set, which after valuation guided the facility design until the main goal: the preliminary design of an academic Ludwieg tube.

Fundamental analyses were conducted on the most expressive key parameters of the facility. The driver Mach number, test section dimensions and test-run duration shall be adequately chosen according to the requirements of importance. In this way, the analyses conducted helped to quantify the stagnation conditions needed to generate approximate flight conditions and the resulting Reynolds number Envelope. In the end, the key parameters where set considering a balance between research potential, safety and feasibility.

The results from the previous analyses aided the guidance of the mechanical project, where a detailed design of the driver section in agreement with ASME design codes was performed. Additionally, the study of existent pulsed wind tunnels provided good insight for formulation and comparison of test section and dump tank concepts. Where a final combination of concepts, judged having more agreement with the proposed requirements, was implemented. Else, the identification of mechanisms, auxiliary equipment and overall engineering solutions applied in each case.

Some of the components still need their own dedicated projects, as it is in the case for the nozzle and fast action valve, although considerations for both components were presented in this work. The nozzle shall be designed with the appropriate numerical method in order to compromise flow quality and exit Mach number in agreement with feasibility. The fast action valve can lead to a more multidisciplinary project.

In conclusion, additionally to the goals accomplished within this project, this work presented a general view of the Ludwieg Tube pulsed facility, trying to cover the most quantity of details as possible. The features of this system as well as the quantity of recent papers found, also related to the design and implementation of this facility on several institutions, strongly indicates that this system could substantially improve the experimental high-speed research in Brazil and the national development of related aerospace technologies. However, paradoxically, not a single work from Brazilian authors about this type of facility was found. That been said, it is believed that this is a pioneer work in the country for this specific subject. This work conceived a preliminary design of the facility. So, there is still many opportunities for future works.

In conclusion, the room for future contributions in this work or even start similar projects from scratch - considering a national application, is vast. Considering the highlight given for the development of novel aerospace high-speed systems in the world and the space for growing projects in this field in Brazil, the motivations for working in this area -but not only limited to pulsed wind tunnels, similarly appears in vast proportions.

BIBLIOGRAPHY

ANDERSON, J. D. **Modern Compressible Flow with Historical Perspective**. 3. ed. New York: McGraw-Hill, 2003. 760 p.

____. Quasi-one-dimensional flow. In: MCGRAW-HILL (eds.). **Modern Compressible Flow with Historical Perspective.** [S.l.]: McGraw-Hill Higher Education, 2003. cap. 5, p. 192–237.

ASME. **Factory-Made Wrought Buttwelding Fittings - ASME B16.9**. New York: The American Society of Mechanical Engineers, 2001.

____. **Metallic Gaskets for Pipe Flanges - ASME B16.20**. New York: The American Society of Mechanical Engineers, 2012.

____. **Pipe Flanges and Flanged Fittings - ASME B16.5**. New York: The American Society of Mechanical Engineers, 2013.

____. **Process Piping - ASME B31.3**. New York: The American Society of Mechanical Engineers, 2016.

____. **ASME Boiler and Pressure Vessel Code, Section II: Materials - Part D: Properties (Metric)**. New York: The American Society of Mechanical Engineers, 2017.

BAKOS, R. J.; ERDOS, J. I. Options for enhancement of the performance of shock-expansion tubes and tunnels. **AIAA 33rd Aerospace Sciences Meeting and Exhibit**, 1995.

BASHOR, I. P.; COMBS, C. S. RANS simulation of the UTSA Mach 7 Ludwieg tube. **AIAA Region IV Student Conference**, 2019.

BASHOR, I. P. et al. Design and preliminary calibration of the UTSA Mach 7 hypersonic Ludwieg tube. **AIAA Aviation Forum**, 2019.

BERTIN, J. J.; CUMMINGS, R. M. Fifty years of hypersonics: where weve been, where were going. **Progress in Aerospace Sciences**, v. 39, n. 6-7, p. 511–536, 2003.

Boom. **XB-1**. 2020. Acessed in Sep. 05, 2020. Disponível em: <https://boomsupersonic.com/xb-1/build>.

BRUN, R. Shock tubes and shock tunnels: Design and experiments. **STO Educational Notes: RTO-EN-AVT-162**, n. 12, p. 24, 2011.

Caltech. **GALCIT Ludwieg Tube**. Caltech Hypesonics Group, 2014. Acesso em 22 ago. 2019. Disponível em: <http://shepherd.caltech.edu/T5/Ae104/Ae104b_handout2014.pdf>.

CHAN, W. Y. K. et al. Aerodynamic design of nozzles with uniform outflow for hypervelocity ground-test facilities. **Journal of Propulsion and Power**, v. 34, n. 6, 2018.

CHUNG, J. **Quasi-One-Dimensional Modeling of an Adiabatic-Compression Preheated Ludwieg Tube**. 2015. 107 p. Dissertação (Master of Science) — University of Maryland, 2015.

CHUNG, J. D.; HOUIM, R. W.; LAURENCE, S. J. Adiabatic-compression preheated Ludwieg tube for the realistic simulation of hypersonic flows. **20th AIAA International Space Planes and Hypersonic Systems and Technologies Conference**, 2015.

CNN Travel. **Concorde's last flight: Is this the greatest aviation photograph of all time?** 2020. Accessed in 05 Sep. 2020. Disponível em: <https://edition.cnn.com/travel/article/concorde-last-flight-photo/index.html>.

CORDIS. **High-Speed Experimental Fly Vehicles - International**. European Commission, 2020. Accessed in 02 Oct. 2020. Disponível em: <https://cordis.europa.eu/project/id/620327>.

CPIHEAT. **SureHeat MAX Air Heater Datasheet**. 2020. Accessed in 3 Aug. 2020. Disponível em: <https://www.cpiheat.com/Sylvania-074734-Sureheat-MAX-Hot-Air-Heater-p/074734.htm>.

CSILLAG, J. M. **Análise do Valor: metodologia do valor**. 4. ed. [S.l.]: Atlas, 1995. 303 p.

CUMMINGS, R. M.; MCLAUGHLIN, T. E. Hypersonic Ludwieg tube design and future usage at the US Air Force Academy. **50th AIAA Aerospace Sciences Meeting including the New Horizons Forum and Aerospace Exposition.**, 2012.

DAVID, K. et al. Aeronautical wind tunnels: Europe and Asia. **Library of Congress Research Report**, 2006.

GILDFIND, D. E.; MORGAN, R. G.; JACOBS, P. A. Expansion tubes in australia. In: IGRA, O.; SEILER, F. (eds.). **Experimental Methods of Shock Wave Research. Shock Wave Science and Technology.** [S.l.]: Springer International Publishing, 2016. cap. 4, p. 399–433.

GNEMMI, P. et al. Shock tunnels at isl. In: IGRA, O.; SEILER, F. (eds.). **Experimental Methods of Shock Wave Research. Shock Wave Science and Technology.** [S.l.]: Springer International Publishing, 2016. cap. 2, p. 131–179.

HICKS, J. W. **Flight Testing of Airbreathing Hypersonic Vehicles**. Dryden Flight Research Facility: NASA Technical Memorandum 4524, 1993.

HOFFMAN, E.; COMBS, C. S. Design considerations and analysis of the UTSA hypersonic Ludwieg tube facility. **AIAA Region IV Student Conference**, 2019.

IGRA, O.; HOUAS, L. Shock tubes. In: IGRA, O.; SEILER, F. (eds.). **Experimental Methods of Shock Wave Research. Shock Wave Science and Technology.** [S.l.]: Springer International Publishing, 2016. cap. 1, p. 3–53.

INCOSE. **Systems Engineering Handbook - A Guide for System Life Cycle Processes and Activities**. 4. ed. [S.l.]: Wiley, 2015. 291 p.

KIMMEL, R. L. et al. AFRL Ludwieg tube initial performance. **55th Aerospace Sciences Meeting**, 2016.

KLICHE, D.; MUNDT, C.; HIRSCHEL, E. The hypersonic mach number independence principle in the case of viscous flow. **Shock Waves**, 2011.

KOPPENWALLNER, G. Hypersonic flow simulation in Ludwieg tube. **Int. Symposium on Recent Advamces in Experimental Fluid Dynamics, IIT Kanpur India.**, 2000.

KOPPENWALLNER, G.; MüLLER-EIGNER, R.; FRIEHMELT, H. Hhk hochschul hyperschall-kanal: Ein "low cost" windkanal für forschung und ausbildung. **DGLR Jahrbuch**, 1993.

LINDORFER, S. A. et al. An investigation of the role of an upstream burst diaphragm on flow quality within a Ludwieg tube using RANS. **46th AIAA Fluid Dynamics Conference**, 2016.

MARTOS, J. F. A. **Investigação Experimental do Veículo Hipersônico Aeroespacial 14-X B**. 2014. 132 p. Dissertação (Master's Degree in Mechanical Engineering) — Universidade Federal do ABC, Santo André, SP, 2014.

MURNAGHAN, M. **Study of minimum length, supersonic nozzle design using the Method of Characteristics**. 2019. 82 p. Dissertação (Master's Degree in Space and Aeronautical Engineering (MASE)) — Universitat Politècnica de Catalunya, 2019.

NASA. **More Pieces of the X-59 are Coming Together**. 2020. Acessed in Sep. 05, 2020. Disponível em: <https://www.nasa.gov/aeroresearch/more-pieces-of-the-x-59-are-coming-together>.

____. **NASAs X-59 Quiet Supersonic Research Aircraft Cleared for Final Assembly**. 2020. Acessed in Jan. 20, 2020. Disponível em: <https://www.nasa.gov/press-release/nasa-s-x-59-quiet-supersonic-research-aircraft-cleared-for-final-assembly>.

OLIVIER, H. The aachen shock tunnel th2 with dual driver mode operation. In: IGRA, O.; SEILER, F. (eds.). **Experimental Methods of Shock Wave Research. Shock Wave Science and Technology.** [S.l.]: Springer International Publishing, 2016. cap. 2, p. 111–131.

PAHL, G. et al. **Projeto na Engenharia Mecânica - Fundamentos do Desenvolvimento Eficaz de Produtos**. 4. ed. [S.l.]: Edgard Blücher, 2005. 407 p.

PARISHER, R. A.; RHEA, R. A. **Pipe Drafting and Design**. 3. ed. [S.l.]: Elsevier, 2012. 470 p.

RADESPIEL, R. et al. Hypersonic Ludwieg tube. In: IGRA, O.; SEILER, F. (eds.). **Experimental Methods of Shock Wave Research. Shock Wave Science and Technology.** [S.l.]: Springer International Publishing, 2016. cap. 4, p. 433–455.

RAO, G. V. R. Exhaust nozzle contour for optimum thrust. **Journal of Jet Propulsion**, v. 28, n. 6, p. 377–382, 1958.

ROMANELLI, D. P. et al. Preliminary characterization of the hypersonic flow in the test section of the IEAv T3 hypersonic shock tunnel. **21st Brazilian Congress of Mechanical Engineering**, p. 10, 2011.

ROMANO, L. N. **Modelo de Referência para o processo de desenvolvimento de Máquinas Agrícolas**. 2003. 321 f. Tese (Doctor's Degree in Mechanical Engineering) — Universidade Federal de Santa Catarina, Santa Catarina, 2003.

SCHRIJER, F. F. J.; BANNINK, W. J. Description and flow assesment of the delft hypersonic Ludwieg tube. **Journal of Spacecraft and Rockets**, v. 47, n. 1, 2010.

SIEMENS. **Additive manufacturing: Better turbines thanks to 3D-printing**. 2020. Accessed in 25 Aug. 2020. Disponível em: <https://new.siemens.com/global/en/company/stories/energy/better-turbines-thanks-to-3d-printing.html>.

SINGH, R. **Optimal Design and Numerical Analisys of Axisymmetric Nozzles**. 2015. 142 f. Monografia (Graduation thesis) — Mechanical Engineering Course, School of Mechanical and Manufacturing Engineering, Sydney, 2015.

TEWARI, A. **Atmospheric and Space Flight Dynamics: Modelling and Simulation with MATLAB and Simulink**. [S.l.]: Birkhäuser, 2006. 567 p.

TORO, P. G. P. et al. Development of a new hypersonic shock tunnel facility to investigate electromagnetic energy addition for flow control and basic supersonic combustion. **American Institute of Physics Conference Proceedings**, v. 860, n. 469, 2006.

____. New hypersonic shock tunnel at the laboratory of aerothermodynamics and hypersonics prof. Henry T. Nagamatsu. **American Institute of Physics Conference Proceedings**, v. 997, n. 1, 2008.

____. Brazilian 14-x hypersonic aerospace vehicle project. **18th AIAA/3AF International Space Planes and Hypersonic Systems and Technologies Conference**, 2012.

____. Projeto da seção de compressão do scramjet acadêmico da UFRN para voo atmosférico acoplado ao foguete de treinamento. **X Congresso Nacional de Engenharia Mecânica**, p. 10, 2018.

USAF. **x-51A Waverider**. US Air Force, 2011. Accessed in 02 Oct. 2020. Disponível em: <https://www.af.mil/About-Us/Fact-Sheets/Display/Article/104467/x-51a-waverider/>.

WIDODO, A. S.; BUTTSWORTH, D. R. Stagnation temperature measurements in the usq hypersonic wind tunnel. **17th Australasian Fluid Mechanics Conference**, 2010.

ÇENGEL, Y. A.; CIMBALA, J. M. **Fluid Mechanics: Fundamentals and Applications**. 3. ed. New York: McGraw-Hill College, 2017. 840 p.

APPENDIX A – MUDGE DIAGRAM

MUDGE DIAGRAM - STAKEHOLDER REQUIREMENTS																								
NEED	1	2					3							4					5					
REQ	1	2	3	4	5	6	7	8	9	10	11	12	13	14	15	16	17	18	19	20	21	**VALUE**	**%**	**Rank**
1		1C	1B	1B	1B	1A	1C	1B	1A	1B	1B	1C	1B	1A	1A	1C	1B	1A	1C	1C	1C	56	9.41	2
2			2C	2B	2B	2A	2B	2B	2A	2A	2B	2C	2B	2A	2A	2A	2A	2A	2C	2C	2C	63	10.59	1
3				3B	3C	3A	3C	3B	3A	3A	3A	3C	3A	3C	3A	3C	3A	3A	3C	3C	3C	54	9.08	4
4					4C	4A	4C	4B	4A	4C	4C	12B	4C	4C	4C	16C	4C	4C	19B	20B	21B	22	3.70	10
5						5A	7B	8B	5B	10C	11C	12A	13A	5C	15B	16B	5C	5B	19B	20B	21B	13	2.18	16
6							7A	8A	9B	10B	11B	12A	13A	14A	15B	16A	17C	18C	19A	20A	21A	0	0.00	21
7								7B	7B	7C	7C	12B	7C	7B	7B	7C	7B	7B	19B	20B	21B	30	5.04	8
8									9A	10C	11C	12A	8C	8C	8B	16B	8C	8C	19B	20B	21B	15	2.52	14
9										10C	9B	12A	13B	14B	9B	16B	9B	9B	19B	20B	21B	20	3.36	12
10											10C	12B	13B	10B	10B	10C	10C	10C	19B	20B	21B	16	2.69	13
11												12A	11B	11C	11B	11C	17C	18C	19A	20A	21A	13	2.18	16
12													12B	12A	12B	12B	12B	12B	19C	20C	21C	54	9.08	4
13														13B	13B	13C	13B	13B	19C	20C	21C	29	4.87	9
14															14B	14C	14C	14C	19B	20B	21B	14	2.35	15
15																16C	17C	18C	19A	20A	21A	6	1.01	18
16																	16B	16B	19A	20A	21A	22	3.70	10
17																		17C	19A	20A	21A	4	0.67	19
18																			19A	20A	21A	3	0.50	20
19																				20C	19C	53	8.91	6
20																					20C	55	9.24	3
21																					21	53	8.91	6
																					TOTAL	595	100.00	

* Read following the Requirement number row. It is compared with another requirement according to the column intersection.

* The number written at the intersections is the "winner" requirement with a relative margin of importance set by the weights.

Weights
A = 5 (much more important)
B = 3 (more important)
C = 1 (little more important)

APPENDIX B – CONCEPTUAL VIEW OF THE PROPOSED FACILITY